Recent progresses in the HAL QCD method for hadron interactions

Sinya Aoki

Center for Gravitational Physics,
Yukawa Institute for Theoretical Physics, Kyoto University

for
HAL QCD collaboration

YITP workshop "QCD phase diagram and lattice QCD"
October 25-29, 2021, Zoom/REMO@YITP, Kyoto

I. Introduction

Hadron interactions in lattice QCD

Finite volume method

spectra of two hadrons in finite box → scattering phase shift

Luescher's finite volume formula

HAL QCD method

NBS wave functions → Potential (Interaction kernel) → scattering phase shift

Schrodinger equation

HAL QCD method

Strategy

NBS wave function

$$\varphi^{\vec{k}}(\vec{x})e^{-W_{\vec{k}}t} = \langle 0|N(\vec{r},t)N(\vec{r}+\vec{x},t)|NN, W_{\vec{k}}\rangle \qquad W_{\vec{k}} = 2\sqrt{\vec{k}^2 + m_N^2}$$

$$\to \sum_{lm} C_{lm} \frac{\sin(kx + \delta_l(k))}{kx} Y_{lm}(\Omega_{\vec{x}})$$

energy-independent non-local potential

$$\left(E_{\vec{k}} - H_0\right)\varphi^{\vec{k}}(\vec{x}) = \int U(\vec{x},\vec{y})\varphi^{\vec{k}}(\vec{y})d^3y, \qquad E_{\vec{k}} = \frac{\vec{k}^2}{m_N}, \;\; H_0 = \frac{-\nabla^2}{m_N},$$

$$W_{\vec{k}} \le W_{\rm th} = 2m_N + m_\pi$$

Derivative expansion $\qquad U(\vec{x},\vec{y}) = V(\vec{x},\vec{\nabla})\delta^{(3)}(\vec{x}-\vec{y})$

$$V(\vec{x},\vec{\nabla}) = V_0(x) + V_\sigma(x)(\vec{\sigma}_1\cdot\vec{\sigma}_2) + V_T(x)S_{12} + V_{\rm LS}(x)\vec{L}\cdot\vec{S} + O(\vec{\nabla}^2)$$

Today's topics

I. Introduction

II. Heavy dibaryons

III. Resonances in the HAL QCD method

IV. HAL QCD potentials in the moving systems

V. Summary and discussions

II. Heavy dibaryons

Y. Lyu, H. Tong, T. Sugiura, S. Aoki, T. Doi, T. Hatsuda, J. Meng, T. Miyamoto,
"Dibaryon with highest charm number near unitarity from lattice QCD",
Phys. Rev. Lett. 127 (2021) 072003 (arXiv:2102.0081).

Baryon (B=1)

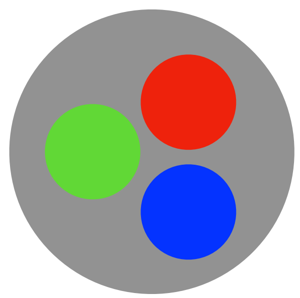

Proton, Neutron,
Lambda, Omega,…

Dibaryon (B=2)

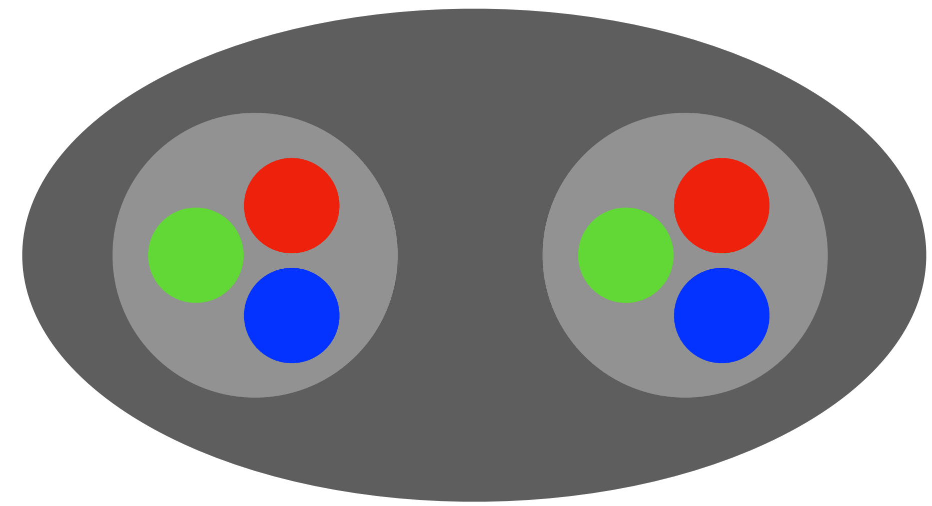

Deuteron
observed in 1930s
+ d*(2380) resonance

Dibaryon = two baryon bound state or resonance

SU(3) classification for Dibaryon candidates (B=2)

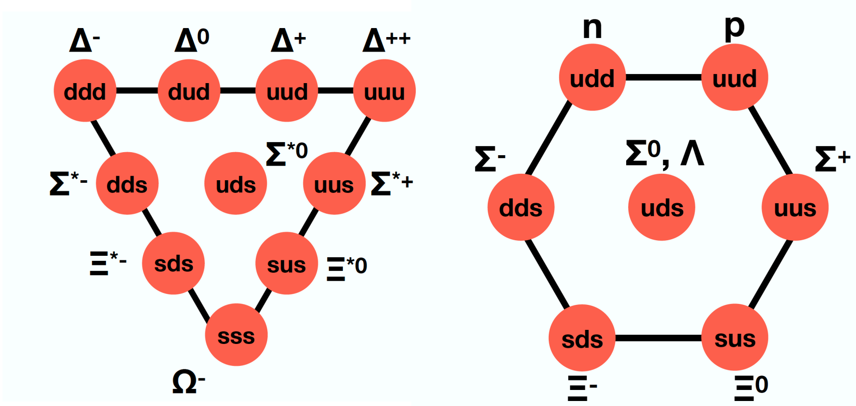

Jaffe (1977)
H-dibaryon(J=0)

1) octet-octet system

$$8 \otimes 8 = 27 \oplus 8_s \oplus \boxed{1} \oplus \boxed{\overline{10}} \oplus 10 \oplus 8_a$$

Deuteron(J=1)

2) decuplet-octet system

NΩ system and NΔ system (J=2)

$$10 \otimes 8 = 35 \oplus \boxed{8} \oplus 10 \oplus 27$$

Goldman et al (1987)
Dyson, Xuong (1964)

3) decuplet-decuplet system

$$10 \otimes 10 = \boxed{28} \oplus 27 \oplus 35 \oplus \boxed{\overline{10}}$$

$d^*(2380)$ resonance

ΩΩ system (J=0)
Zhang et al(1997)

ΔΔ system (J=3)
Dyson, Xuong (1964)
Kamae, Fujita(1977)
Oka, Yazaki(1980)

Previous results

H dibaryon

T. Inoue et al. (HAL QCD Coll.), PRL106(2011)162002 — flavor SU(3) limit

K. Sasaki et al. (HAL QCD Coll.), NPA106(2020)121737 — physical point, $\Lambda\Lambda, N\Xi$

$\Delta\Delta$ dibaryons

S. Gongyo et al. (HAL QCD Coll.), PLB811(2020)135935 — flavor SU(3) limit, $d^*(2380)$

$N\Omega$ dibaryons

F. Etminan et al. (HAL QCD Coll.), NPA928(2014)89 — $m_\pi \simeq$ 875 MeV

T. Iritani et al. (HAL QCD Coll.), PLB792(2019)284 — physical point

$\Omega\Omega$ dibaryons

M. Yamada et al. (HAL QCD Coll.), PTEP 7(2015)187 — $m_\pi \simeq$ 700 MeV

S. Gongyo et al. (HAL QCD Coll.), PRL 120(2018)212001 — physical point

$\Omega_{ccc}\Omega_{ccc}$ dibaryons

Y. Lyu, et al., Pays. Rev. Lett. 127 (2021) 072003 (arXiv:2102.0081)

$\Omega(ccc)$: triply charmed baryon, stable against strong decay, mass/EM form factor

$\Omega(ccc)\Omega(ccc)$: S-wave& zero total spin, then no Pauli exclusion

↓

attractions ?

↓

bound state ?

HAL QCD method

R-correlator

$$R(\boldsymbol{r}, t>0) = \langle 0|\Omega_{ccc}(\boldsymbol{r},t)\Omega_{ccc}(\boldsymbol{0},t)\overline{\mathcal{J}}(0)|0\rangle / e^{-2m_{\Omega_{ccc}}t}$$
$$= \sum_n A_n \psi_n(\boldsymbol{r}) e^{-(\Delta W_n)t} + O(e^{-(\Delta E^*)t}),$$

non-local potential

$$\left(\frac{1}{4m_{\Omega_{ccc}}}\frac{\partial^2}{\partial t^2} - \frac{\partial}{\partial t} - H_0\right) R(\boldsymbol{r},t) = \int d\boldsymbol{r}' U(\boldsymbol{r},\boldsymbol{r}') R(\boldsymbol{r}',t),$$

derivarive expansion $U(\mathbf{r},\mathbf{r}') = V(\mathbf{r})\delta^{(3)}(\mathbf{r}-\mathbf{r}') + \cdots$

local potential

$$V(r) = R^{-1}(\boldsymbol{r},t)\left(\frac{1}{4m_{\Omega_{ccc}}}\frac{\partial^2}{\partial t^2} - \frac{\partial}{\partial t} - H_0\right) R(\boldsymbol{r},t).$$

at reasonably large t

Lattice setup

2+1 flavor gauge configuration on 96^4 lattice

with Iwasaki gauge + NP $O(a)$ improved clover quark

$a \simeq 0.0846$ fm, $m_\pi \simeq 146$ MeV, $m_K \simeq 525$ MeV (near physical point)

$La \simeq 8.1$ fm

(quenched) charm quark mass

	$(m_{\eta_c} + 3m_{J/\Psi})/4$ [MeV]	$m_{\Omega_{ccc}}$ [MeV]
set 1	3096.6(0.3)	4837.3(0.7)
set 2	3051.4(0.3)	4770.2(0.7)
Interpolation	3068.5(0.3)	4795.6(0.7)
Exp.	3068.5(0.1)	-

potential → scattering phase shift

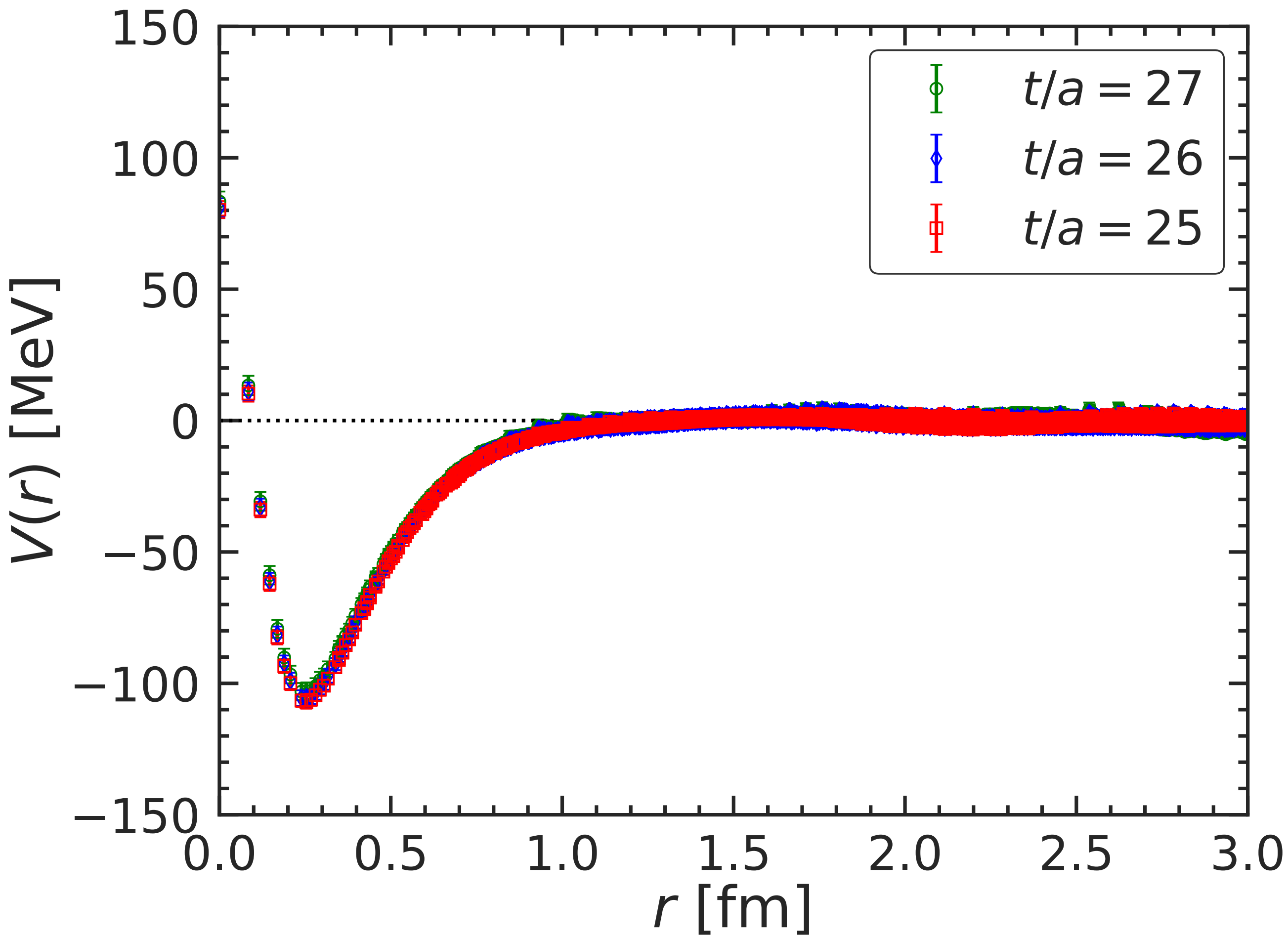

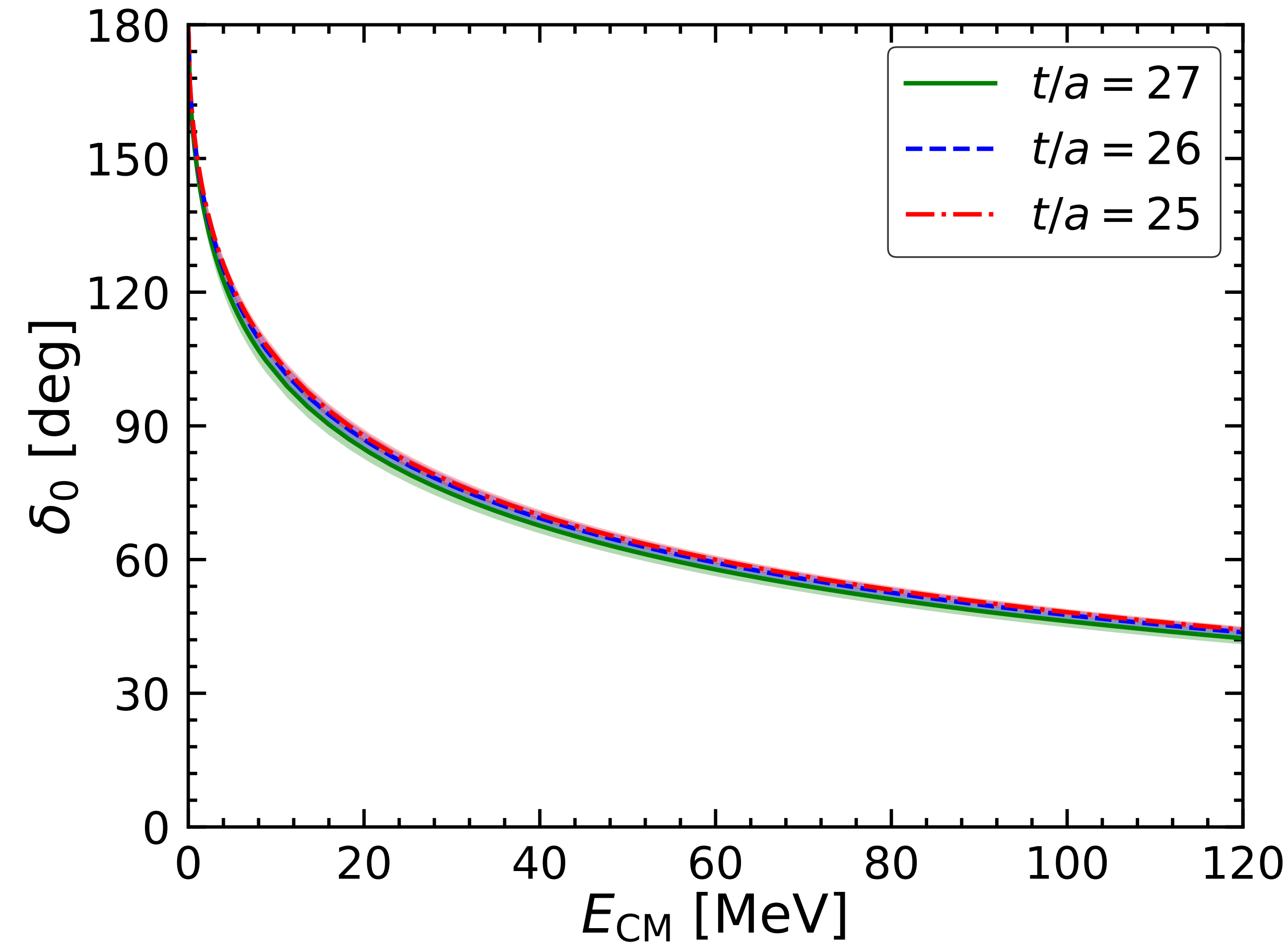

one bound state

$$B = 5.68(0.77)(^{+0.46}_{-1.02}) \text{ MeV}, \quad \text{BE}$$

$$\sqrt{\langle r^2 \rangle} = 1.13(0.06)(^{+0.08}_{-0.03}) \text{ fm}. \quad \text{size}$$

Effective Range Expansion (ERE)

$$k \cot \delta_0(k) = -\frac{1}{a_0} + \frac{1}{2} r_{\text{eff}} k^2 + O(k^4)$$

scattering length

$$a_0 = 1.57(0.08)(^{+0.12}_{-0.04}) \text{ fm},$$

$$r_{\text{eff}} = 0.57(0.02)(^{+0.01}_{-0.00}) \text{ fm}.$$

effective range

$$B = \frac{(1 - \sqrt{1 - 2r_{\text{eff}}/a_0})^2}{m_{\Omega_{ccc}} r_{\text{eff}}^2} \simeq 5.7 \text{ MeV}$$

$$\sqrt{\langle r^2 \rangle} = \frac{a_0}{\sqrt{2}} \simeq 1.1\text{fm}$$

← loosely bound state

Coulomb repulsion

charge distribution inside Ω_{ccc}

$$\rho(r) = \frac{12\sqrt{6}}{\pi r_d^3} \exp\left[-\frac{2\sqrt{6}r}{r_d}\right]$$

charge radius of Ω_{ccc} $\quad r_d = 0.410(6)$ fm

K. U. Can, et al., Phys. Rev. D92 (2015) 114515.

Coulomb potential between two Ω_{ccc} 's

$$V^{\mathrm{Coulomb}}(r) = \alpha_e \iint d^3r_1 d^3r_2 \frac{\rho(r_1)\rho(|\vec{r}_2 - \vec{r}|)}{|\vec{r}_1 - \vec{r}_2|}$$

ERE with Coulomb

$$k\left[C_\eta^2 \cot\delta_0^{\mathrm{C}}(k) + 2\eta h(\eta)\right] = -\frac{1}{a_0^{\mathrm{C}}} + \frac{1}{2} r_{\mathrm{eff}}^{\mathrm{C}} k^2 + O(k^4),$$

$$C_\eta^2 = \frac{2\pi\eta}{e^{2\pi\eta}-1}, \quad \eta = 2\alpha_e m_{\Omega_{ccc}}/k,$$

$$h(\eta) = \mathrm{Re}[\Psi(i\eta)] - \ln(\eta)$$

$\Psi(x)$: digamma function

$1/a_0^C$ vs. $\alpha_e/\alpha_e^{\text{phys.}}$

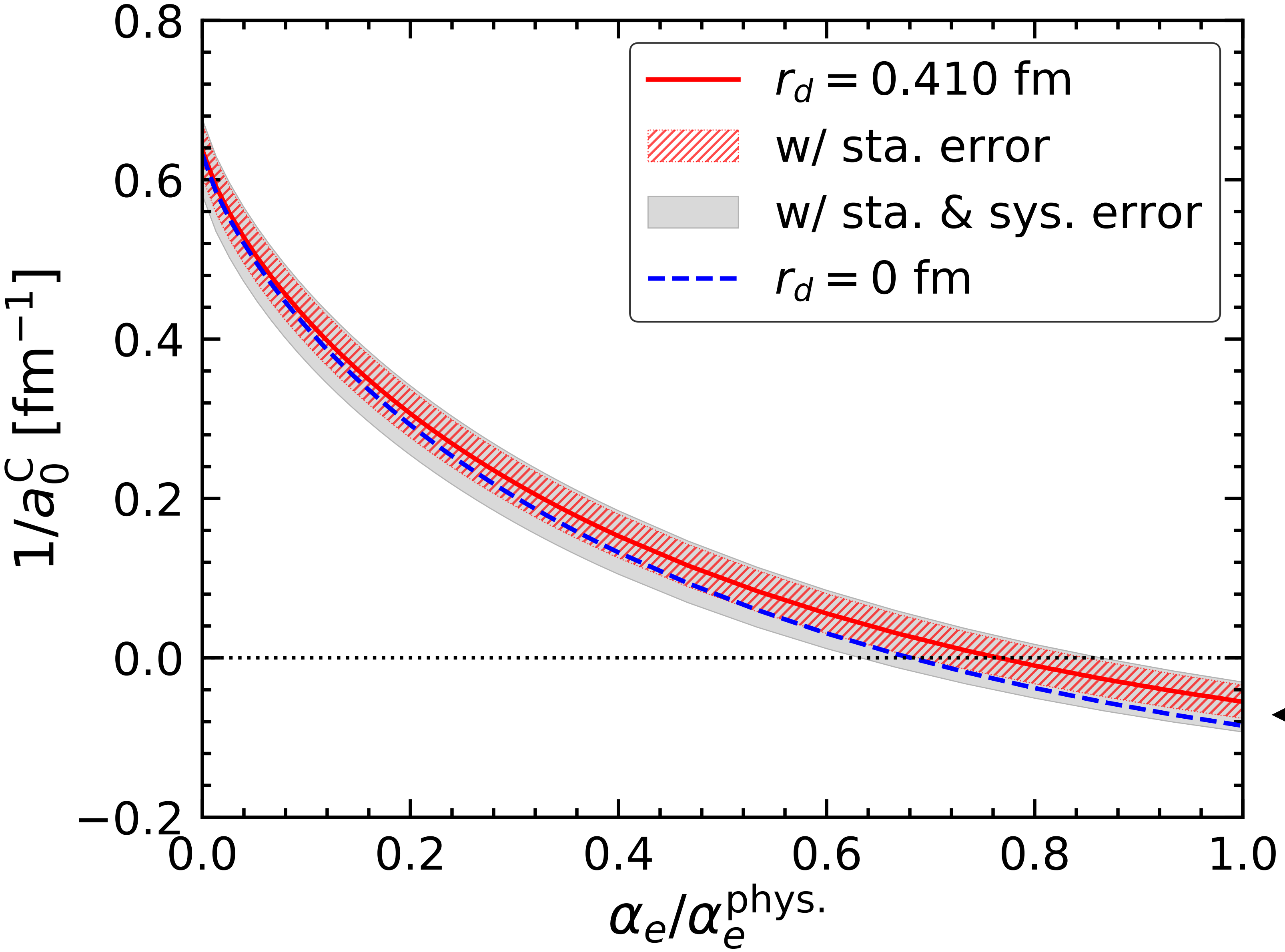

physical value

$$a_0^{\mathrm{C}} = -19(7)\left(^{+7}_{-6}\right)\ \mathrm{fm},$$

unitary region

$$r_{\mathrm{eff}}^{\mathrm{C}} = 0.45(0.01)\left(^{+0.01}_{-0.00}\right)\ \mathrm{fm}.$$

$r_{\text{eff}}^C/a_0^C = -0.024(0.010)(^{+001}_{-0.00})$ fm

Comparison with other dibaryons

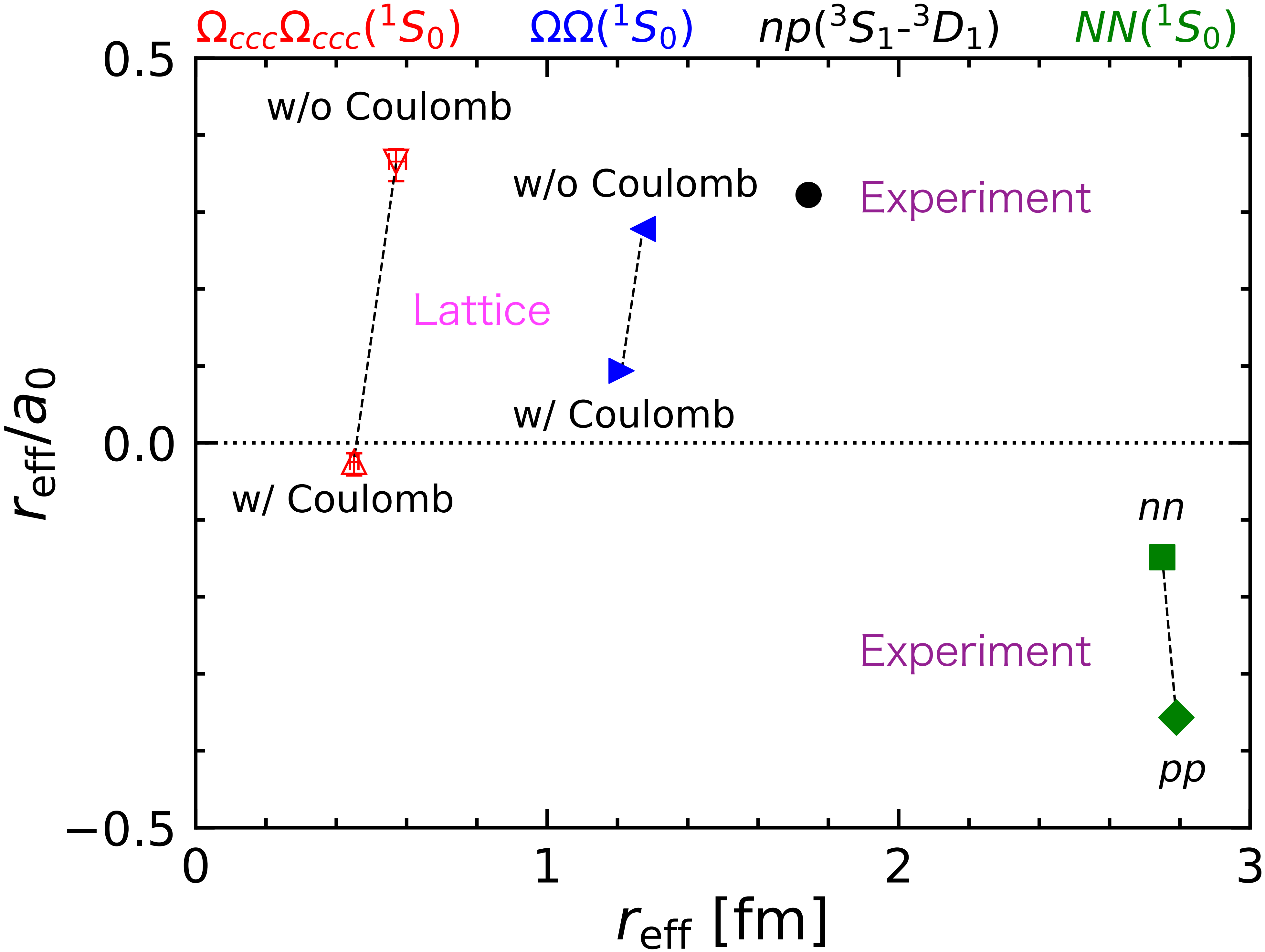

All “dibaryons” appear near unitarity. Why ?

$\Omega_{ccc}\Omega_{ccc}(^1S_0)$ dibaryon is closest to unitarity among these.

III. Resonance in the HAL QCD method

Y. Akahoshi, S. Aoki, T. Doi,

“Emergence of ρ resonance from the HAL QCD potential in lattice QCD”,

Phys. Rev. D104 (2021) 054510 (arXiv:2106.08173).

ρ resonance

ρ meson is a resonance of $\pi\pi$ scattering

Can we reproduce ρ resonance form $I = 1$ $\pi\pi$ HAL QCD potential ?

Obstructions/Difficulties

"box" diagram for $I = 1$ $\pi\pi$ system

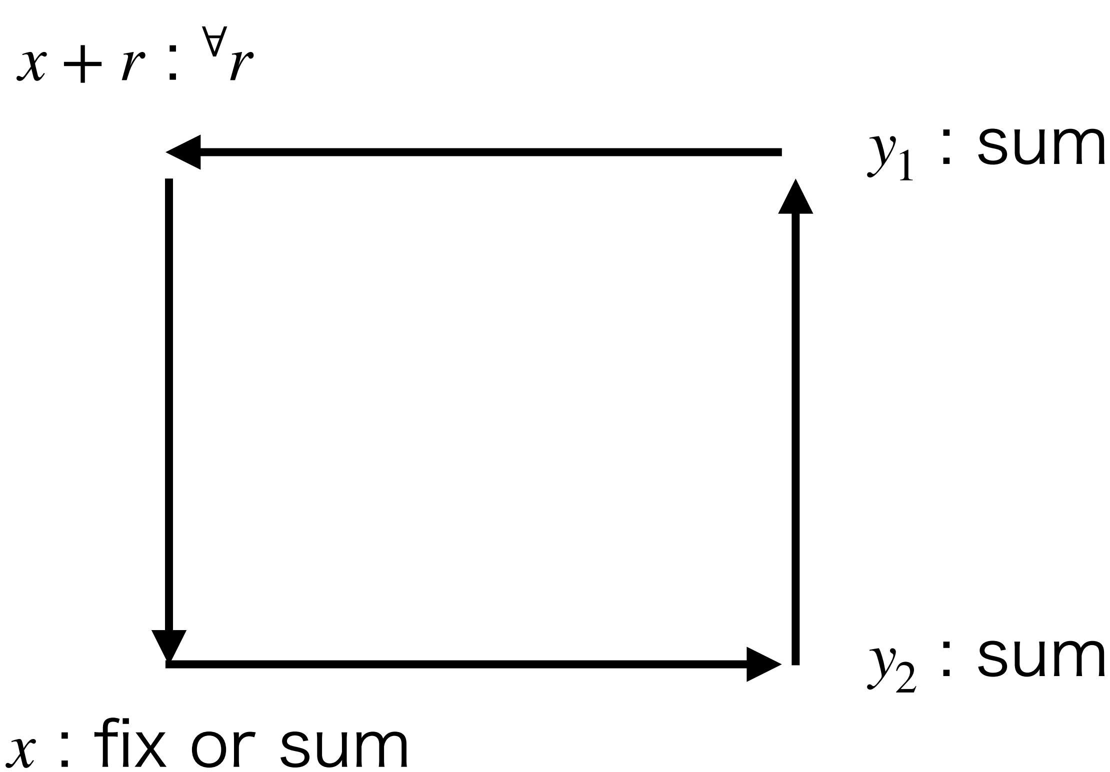

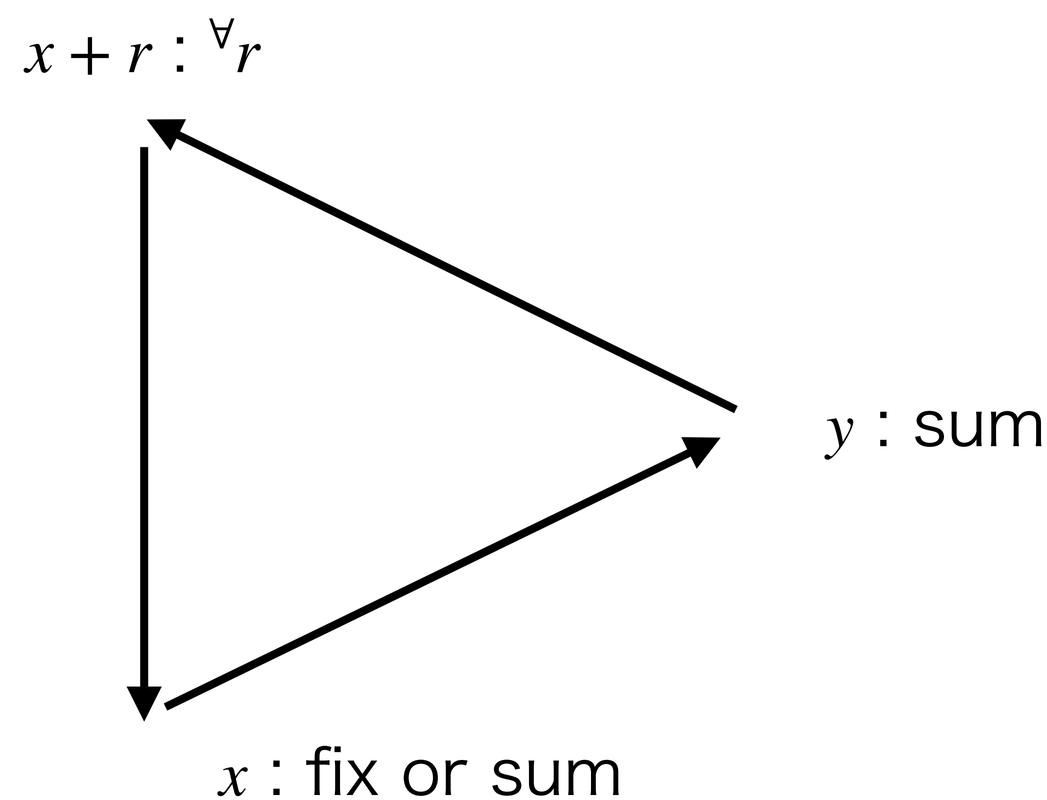

several all-to-all propagators are needed. → large numerical cost/noises

Our strategy

3 techniques for all-to-all propagators are combined.

- one-end trick — C. McNeill, C. Michael, PRD73 (2006) 074506.
- sequential propagator — G. Martinelli, C.T. Sachrajda, NPB316 (1989) 355.
- covariant approximation averaging (CAA) — E. Shintani, et al, PRD91 (2015) 114511.

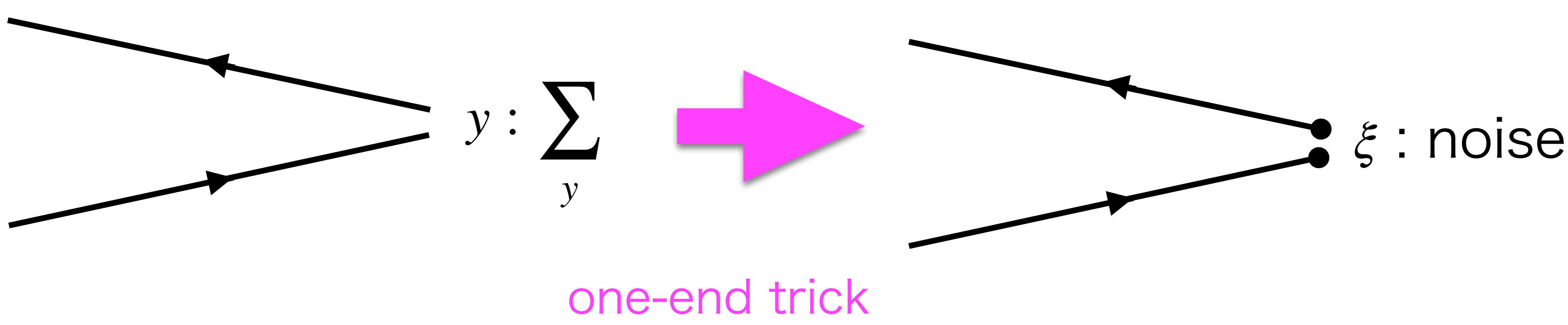

two (ρ and $\pi\pi$) sources → N^{2}LO analysis

smeared sink operators → remove short distance singularity expected by OPE

Diagrams

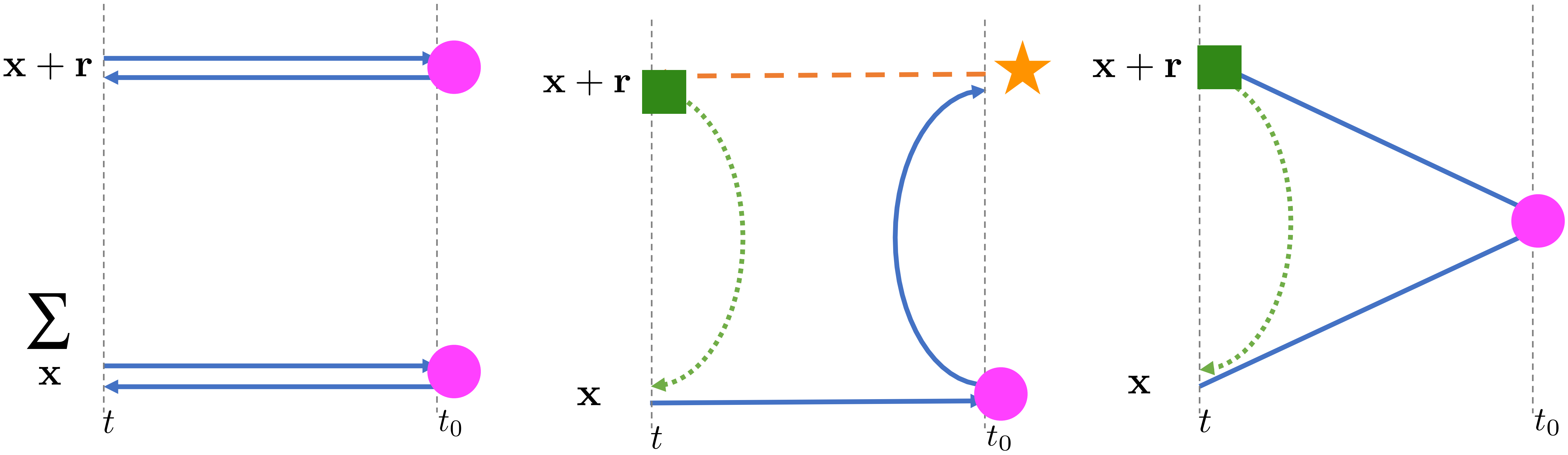
$\mathbf{x}+\mathbf{r}$
$\sum_{\mathbf{x}}$
t
t_0
$\mathbf{x}+\mathbf{r}$
$\mathbf{x}$
t
t_0
$\mathbf{x}+\mathbf{r}$
$\mathbf{x}$
t
t_0

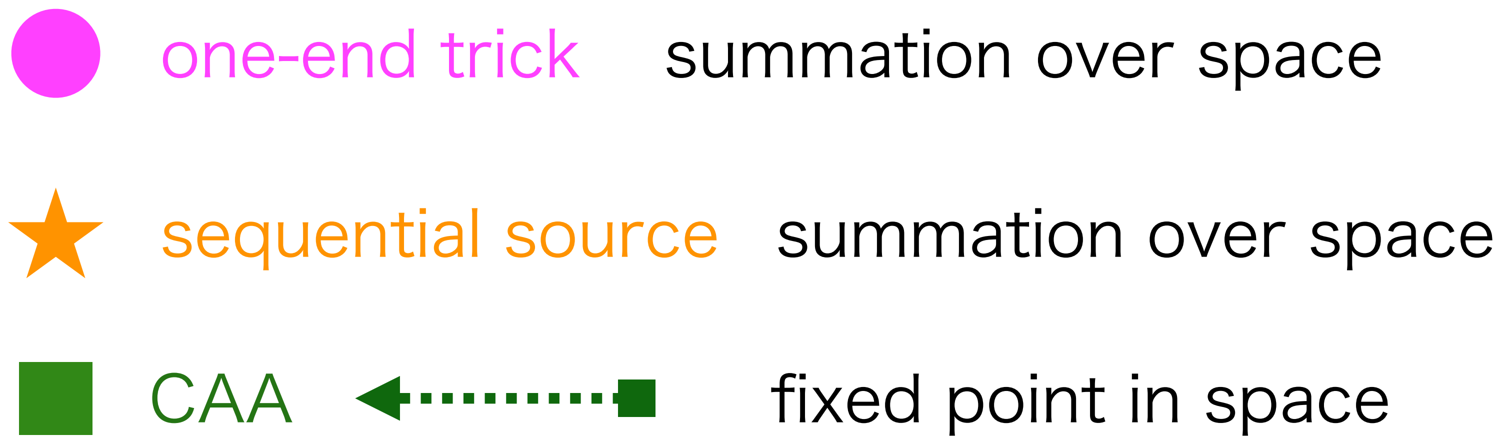
one-end trick
summation over space
sequential source
summation over space
CAA
fixed point in space

Lattice setup

2+1 flavor gauge configuration on $32^3 \times 64$ lattice

with Iwasaki gauge + NP $O(a)$ improved clover quark

$a \simeq 0.0907$ fm, $m_\pi \simeq 411$ MeV, $m_\rho \simeq 892$ MeV (PACS-CS configurations)

$La \simeq 2.9$ fm

statistics

Source type	Scheme	$N_{\rm conf}$ (#. of time slice ave.)	Stat. error
$\pi\pi$-type	equal-time, smeared-sink	100 (64)	jackknife with bin–size 5
ρ-type	equal-time, smeared-sink	200 (64)	jackknife with bin–size 10

one-end trick and CAA

Source type	One-end trick		CAA	
	Noise vector	Space dilution	$N_{\rm eig}$	# of averaged points
$\pi\pi$-type	Z_4 noise	$s2$ (even-odd)	300	64
ρ-type	Z_4 noise	$s4$	300	64

Results

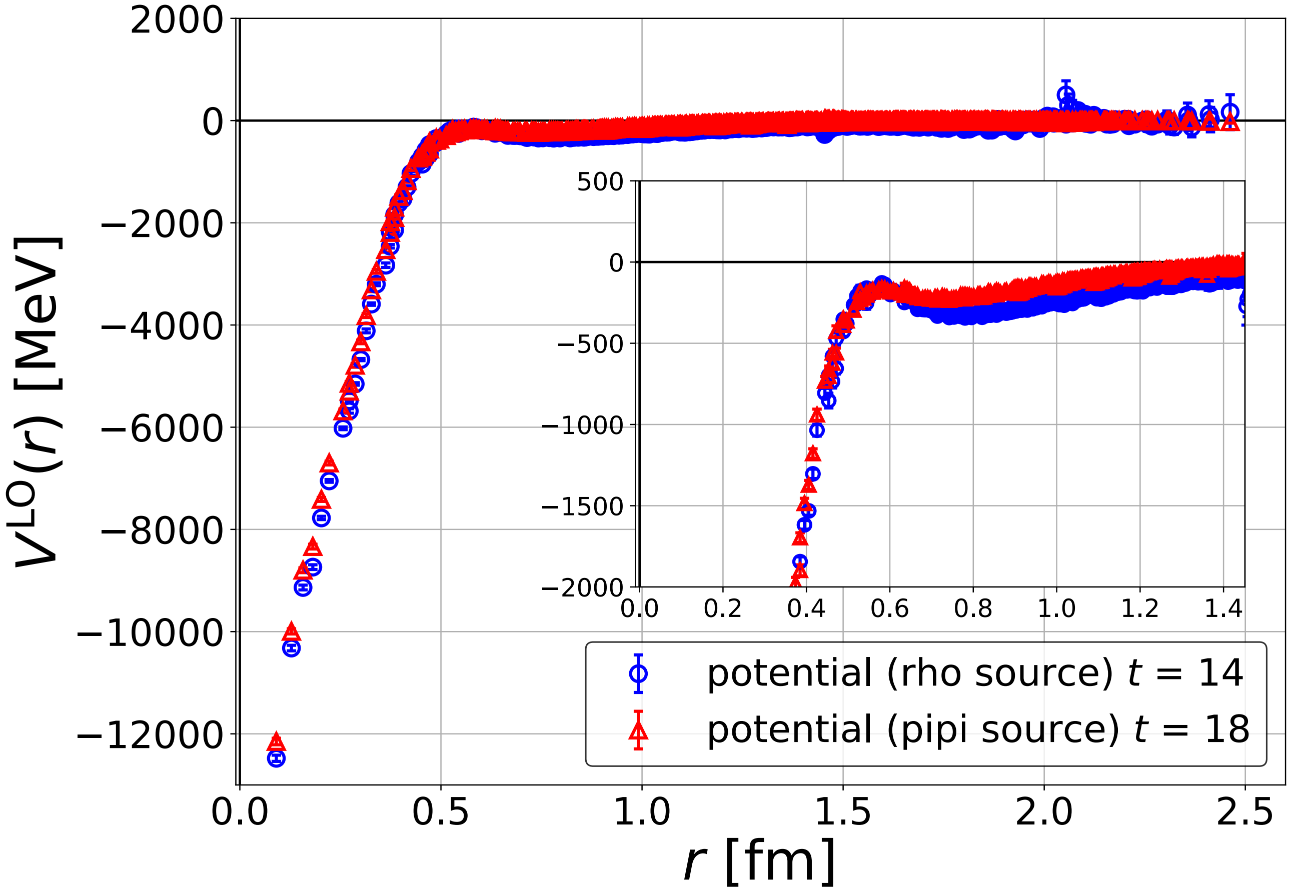

Leading order potentials from ρ and $\pi\pi$ sources

Higher partial waves are reduced

T. Miyamoto, et al, PRD101 (2020) 074514.

+ L=1 centrifugal term

$$V_C(r) = \frac{1}{2\mu}\frac{L(L+1)}{r^2}$$

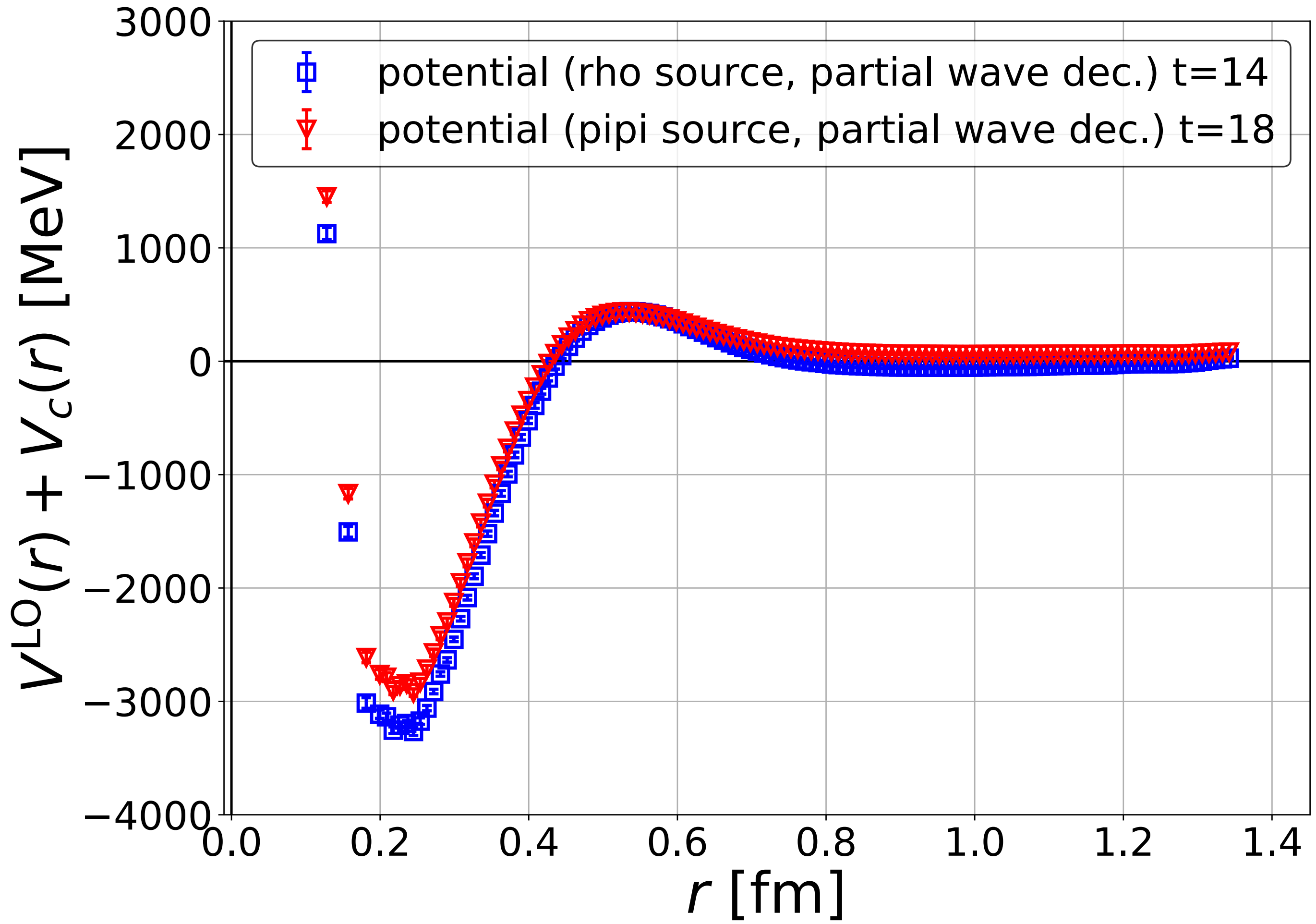

phase shift

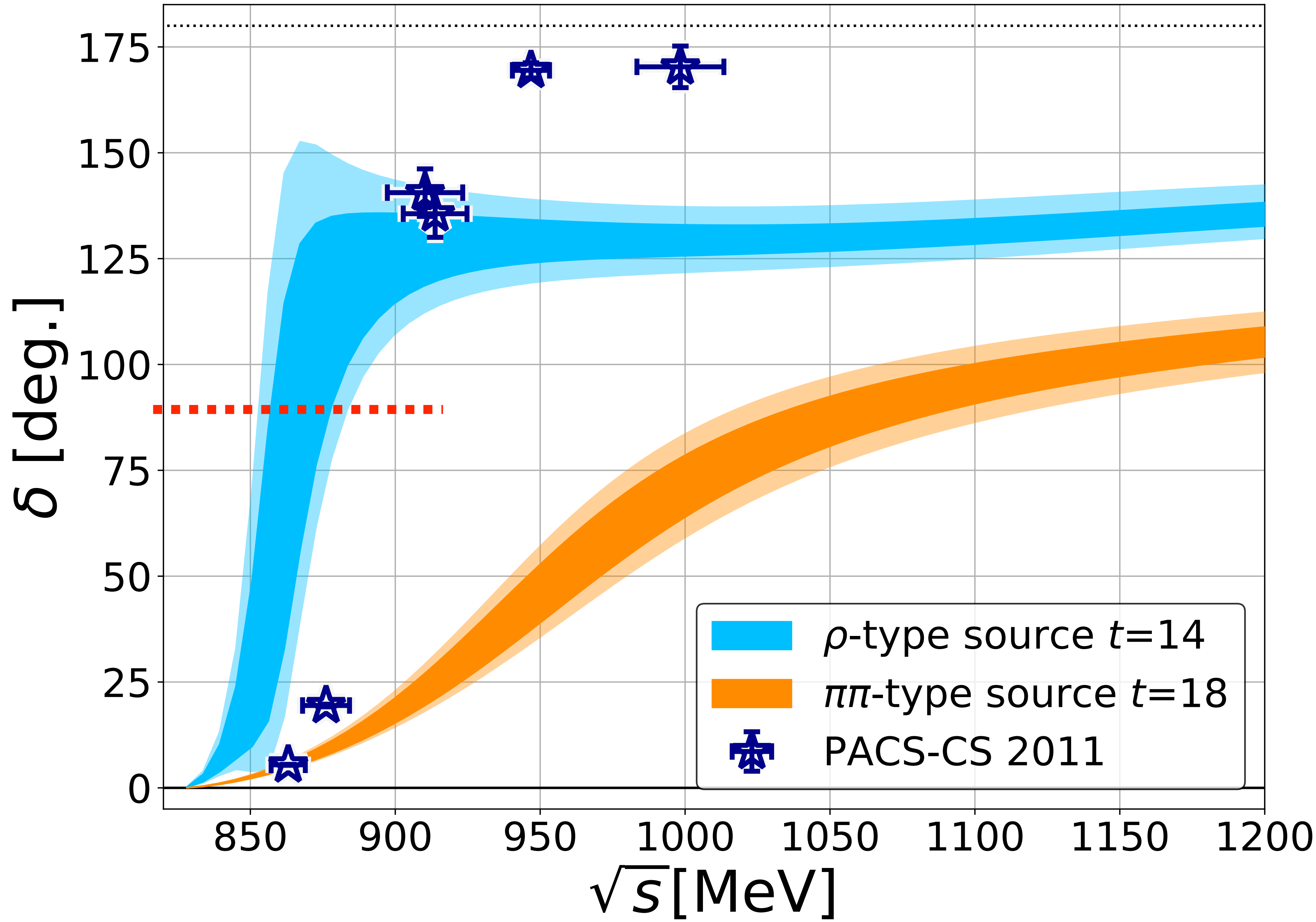

resonant behaviors are seen.

results from two sources differ. → N²LO analysis is mandatory.

they disagree with the FV spectra.

N²LO potential

$$U^{\mathrm{N^2LO}}(\mathbf{r},\mathbf{r}') = \left(V_0^{\mathrm{N^2LO}}(r) + V_2^{\mathrm{N^2LO}}(r)\,\nabla^2 \right) \delta(\mathbf{r}-\mathbf{r}')$$

$V_0^{\mathrm{N^2LO}}(r)$

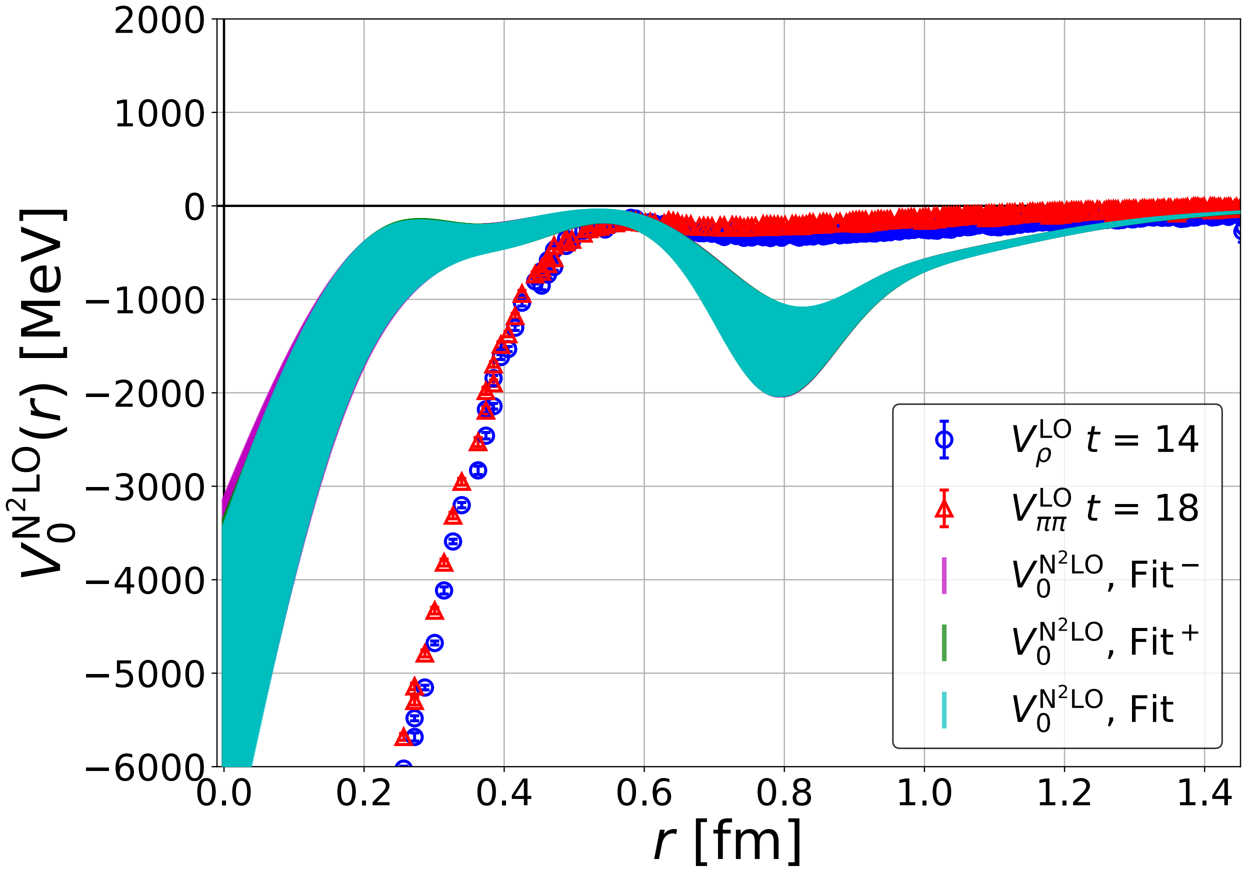

$V_2^{\mathrm{N^2LO}}(r)$

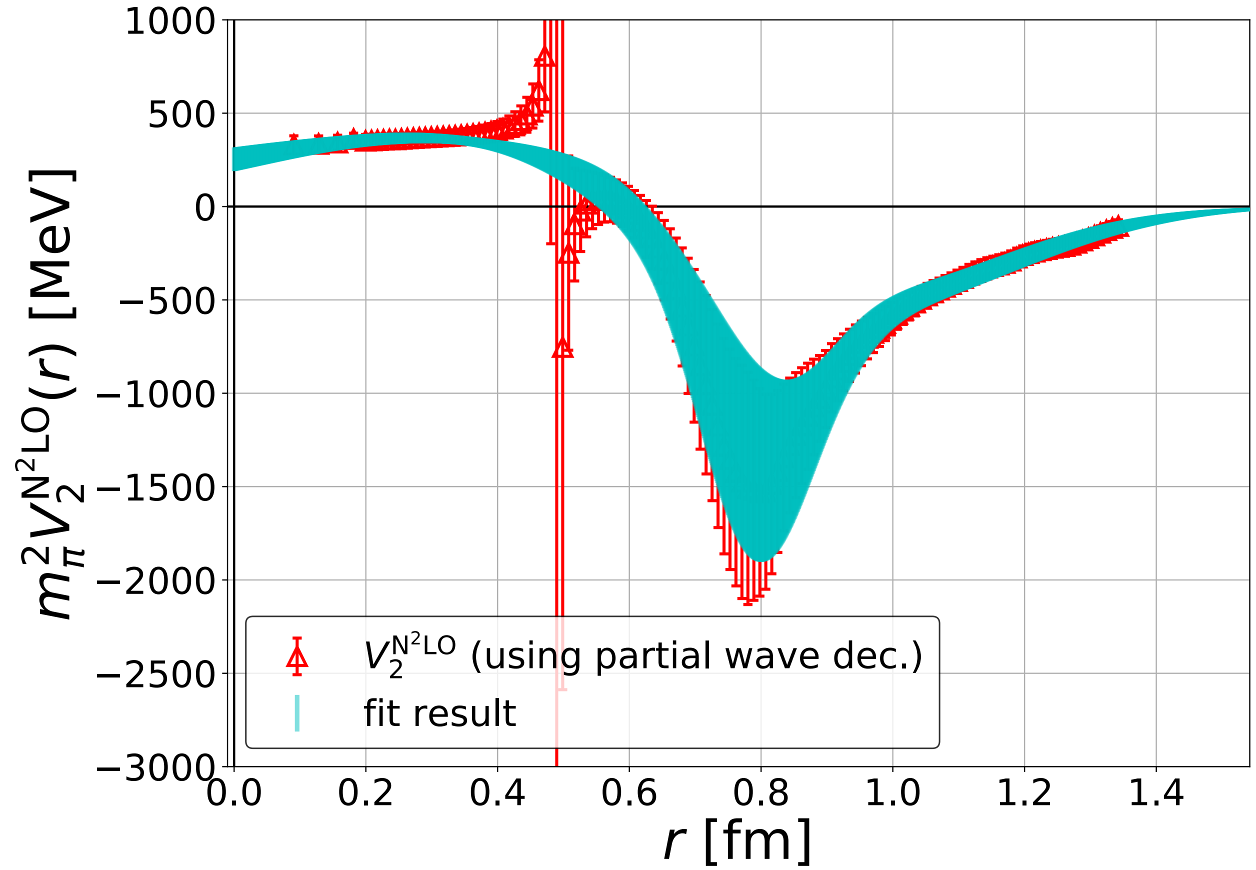

$V_0^{\mathrm{N^2LO}}(r)$ is obtained. ← $V_2^{\mathrm{N^2LO}}(r)$ with large noises is fitted first.

cf. a singularity could be included.

S. Aoki, K. Yazaki, arXiv:2109.07665(hep-lat).

N^{2}LO phase shift

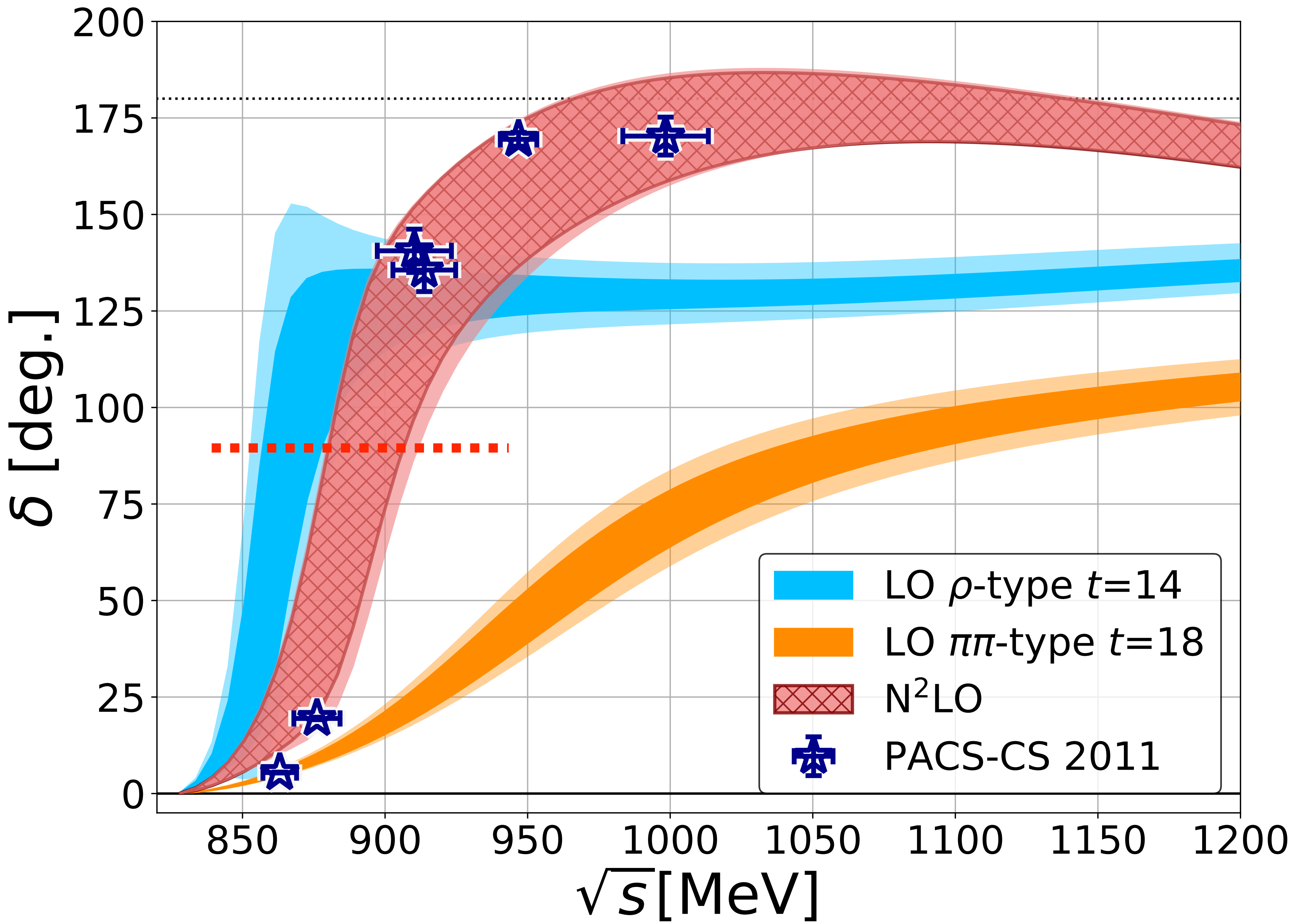

N2LO result almost agrees with the PACS-CS by the FV method.

ρ resonance parameters

Breit-Wigner fit $$\frac{k^3 \cot \delta_1(k)}{\sqrt{s}} = \frac{6\pi}{g^2_{\rho\pi\pi}}(m^2_\rho - s),$$

pole of the S-matrix from N²LO potential

both agree well.

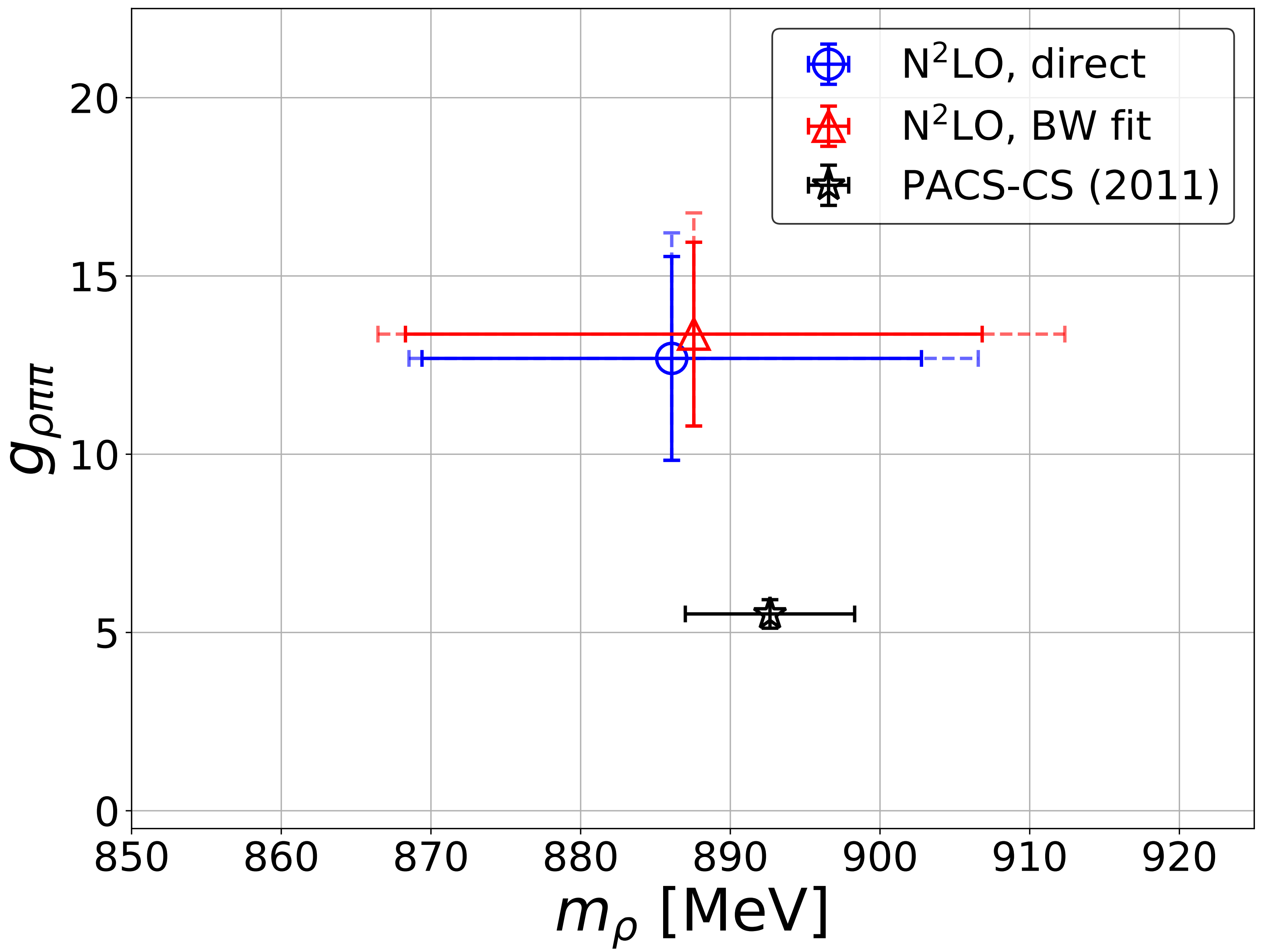

m_ρ from potential agrees with the PACS-CS (FV), while $g_{\rho\pi\pi}$ is much larger.

Why $g_{\rho\pi\pi}$ is larger ?

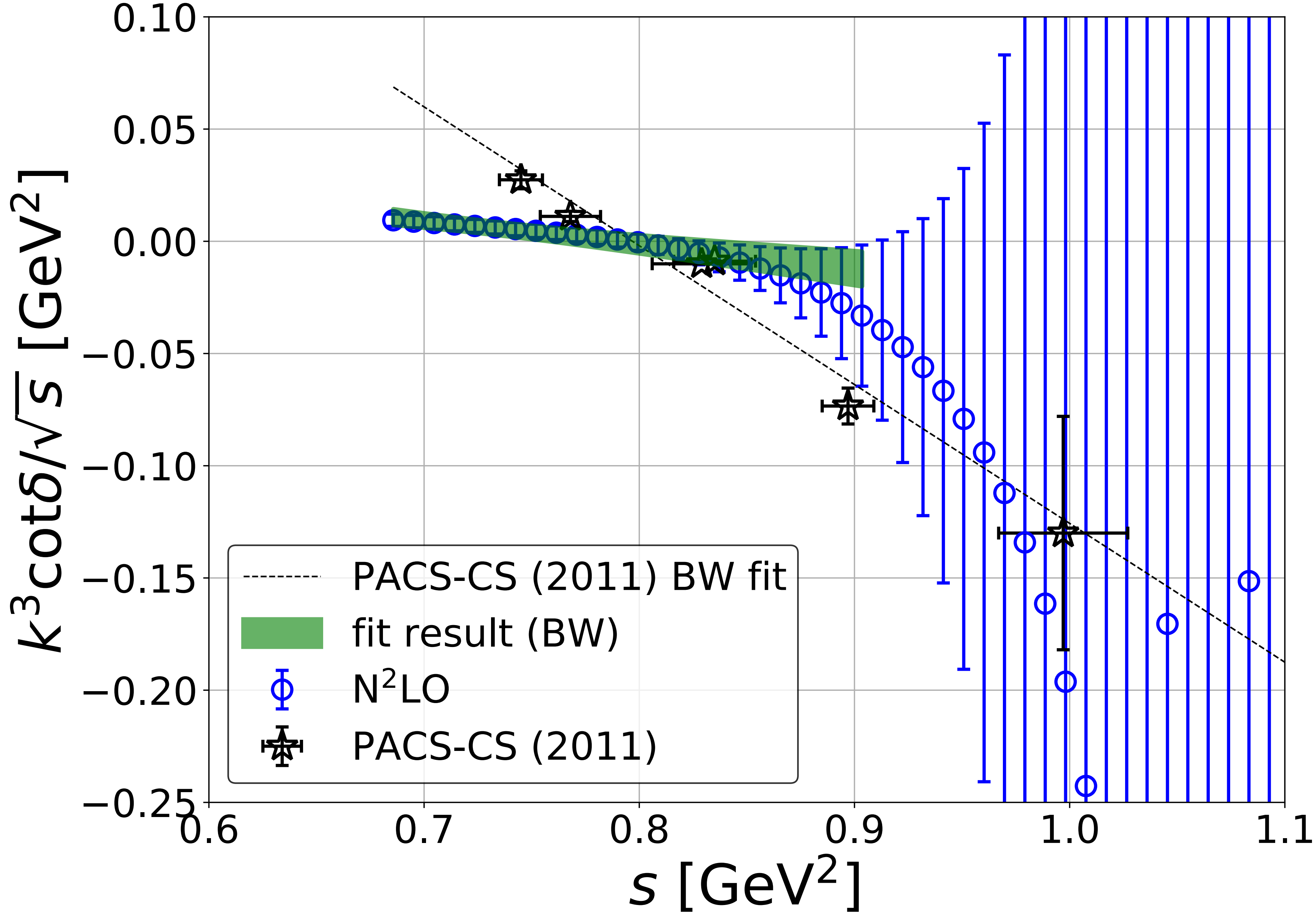

$$\frac{k^3 \cot \delta_1(k)}{\sqrt{s}} = \frac{6\pi}{g^2_{\rho\pi\pi}}(m^2_\rho - s),$$

slope is smaller for the potential result.

Probably, the lack of low s states in the center of mass causes this behavior.

IV. HAL QCD potentials in the moving system

Y. Akahori and S. Aoki, in preparation.

σ resonances

σ resonance from $\pi\pi$ scattering in the center of mass system

$$\langle 0|\pi(t)\pi(t)\sigma(0)|0\rangle \simeq \underline{\langle 0|\pi(t)\pi(t)|0\rangle}\langle 0|\sigma(0)|0\rangle + e^{-E_{\pi\pi}t}\langle 0|\pi(t)\pi(t)|\pi\pi\rangle\langle\pi\pi|\sigma(0)|0\rangle$$

vacuum states dominates signals

↓ **non-zero total momentum (boosted system)**

$$\langle 0|\pi(t)\pi(t)\sigma(0)|0\rangle \simeq e^{-E_{\pi\pi}t}\langle 0|\pi(t)\pi(t)|\pi\pi\rangle\langle\pi\pi|\sigma(0)|0\rangle + \cdots$$

vacuum contribution is absent

HAL QCD method was formulated for a boosted system. S. Aoki, Lattice 2019.

Recently, numerical test for $I = 2$ $\pi\pi$ system has been performed.

IV-1. Theory

S. Aoki, lattice 2019.

Setup

Center of mass (CM)

$(E_k, \mathbf{k})$ $\quad$ $(E_k, -\mathbf{k})$

$$\mathbf{P}^* = 0 \qquad E_k = \sqrt{\mathbf{k}^2 + m^2}$$

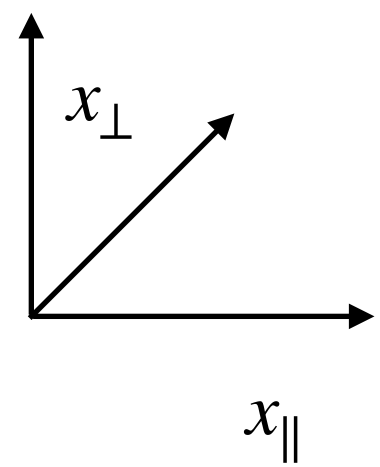

Moving

x_1 $\quad$ x_2

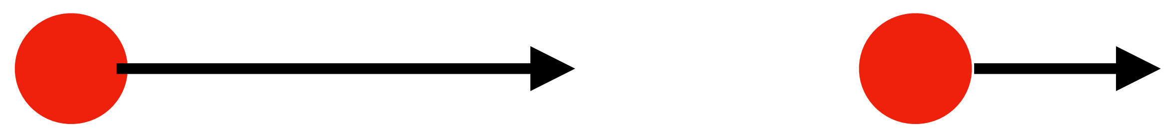

$$\mathbf{P} = \mathbf{k}_1 + \mathbf{k}_2$$

$(E_{k_1}, \mathbf{k}_1)$ $\quad$ $(E_{k_2}, \mathbf{k}_2)$

Lorentz transformation

$$\mathbf{P}^* = \gamma(\mathbf{P} - \mathbf{v}W) = 0 \qquad W = \sqrt{\mathbf{k}_1^2 + m^2} + \sqrt{\mathbf{k}_2^2 + m^2} \qquad \gamma := \frac{1}{\sqrt{1 - \mathbf{v}^2}}$$

$$P \cdot X = P^* \cdot X^* \qquad X := \frac{x_1 + x_2}{2}, x := x_1 - x_2$$

HAL QCD potential from boosted NBS wave function

Leading order HAL QCD potential

$$V^{\rm LO}_{x^{*4}}(\mathbf{x}^*) = \frac{(\nabla^{*2} + k^{*2})\varphi_{k_1^*,k_2^*}(\mathbf{x}^*, x^{*4})}{2\mu\varphi_{k_1^*,k_2^*}(\mathbf{x}^*, x^{*4})}.$$

CM

NBS wave function

$$e^{iP\cdot X}\varphi_{k_1,k_2}(x) = e^{iP^*\cdot X^*}\varphi_{k_1^*,k_2^*}(x^*)$$

Moving CM

$$x^{*4} = \gamma(x^4 - i\mathbf{v}\cdot\mathbf{x}_\parallel), \quad \mathbf{x}^*_\parallel = \gamma(\mathbf{x}_\parallel + i\mathbf{v}x^4), \quad \mathbf{x}^*_\perp = \mathbf{x}_\perp.$$

LO potential $x^4 = \mathbf{x}_\parallel = 0$

Moving

$$V^{\rm LO}_{x^{*4}=0}(\mathbf{x}^*_\perp) = \left.\frac{(\nabla_\perp^2 + \gamma^2(\nabla_\parallel + i\mathbf{v}\partial_{x^4})^2 + k^{*2})\varphi_{k_1,k_2}(\mathbf{x}, x^4)}{2\mu\varphi_{k_1,k_2}(\mathbf{x}, x^4)}\right|_{x^4=0,\mathbf{x}_\parallel=0}$$

CM Moving

Time dependent method

CM
$$\left(-H_0 - \partial_{X^{*4}} + \frac{1}{4m}\partial^2_{X^{*4}}\right) R(\mathbf{x}^*, x^{*4}, X^{*4}) = V^{\mathrm{LO}}_{x^{*4}}(\mathbf{x}^*) R(\mathbf{x}^*, x^{*4}, X^{*4})$$

$$R(\mathbf{x}^*, x^{*4}, X^{*4}) := \sum_n B_n \varphi_{W_n^*}(x^*) e^{-\underline{(W_n^*-2m)}X^{*4}} + \cdots$$

NBS

Moving
$$R(\mathbf{x}, x^4, X^4) \simeq \sum_n B_n \varphi_{W_n}(x) e^{-(W_n-2m)X^4}$$

$$V^{\mathrm{LO}}_{x^{*4}=0}(\mathbf{x}_\perp) = \left. \frac{\left(L_\perp + L_\parallel + mE\right)(\mathbf{x}, x^4, X^4)}{mG(\mathbf{x}, x^4, X^4)} \right|_{x^4=0, \mathbf{x}_\parallel=0}$$

$$G(\mathbf{x}, x^4, X^4) = \left((\partial_{X^4} - 2m)^2 - \mathbf{P}^2\right) R(\mathbf{x}, x^4, X^4),$$

$$E(\mathbf{x}, x^4, X^4) = \left[\partial^2_{X^4}/4m - \partial_{X^4} - \mathbf{P}^2/4m\right] G(\mathbf{x}, x^4, X^4),$$

$$L_\perp(\mathbf{x}, x^4, X^4) = \nabla^2_\perp G(\mathbf{x}, x^4, X^4),$$

$$L_\parallel(\mathbf{x}, x^4, X^4) = \left(-(\partial_{X^4} - 2m)\nabla_\parallel + i\mathbf{P}\partial_{x^4}\right)^2 R(\mathbf{x}, x^4, X^4).$$

IV-2. Numerical results

$I = 2 \; \pi\pi$ potential

Akahoshi and Aoki, in preparation.

Numerical setup

$2+1$ flavor CP-PACS configurations on a $32^3 \times 64$ latttice

Iwasaki gauge action and non-perturbatively improved Wilson quark action

$a \simeq 0.0907$ fm, $m_\pi \simeq 700$ MeV

smeared quark source

case1: $\mathbf{P} = (0, 0, 2\pi/L)$,

case2: $\mathbf{P} = (0, 0, 4\pi/L)$,

CM: $\mathbf{P} = (0, 0, 0)$,

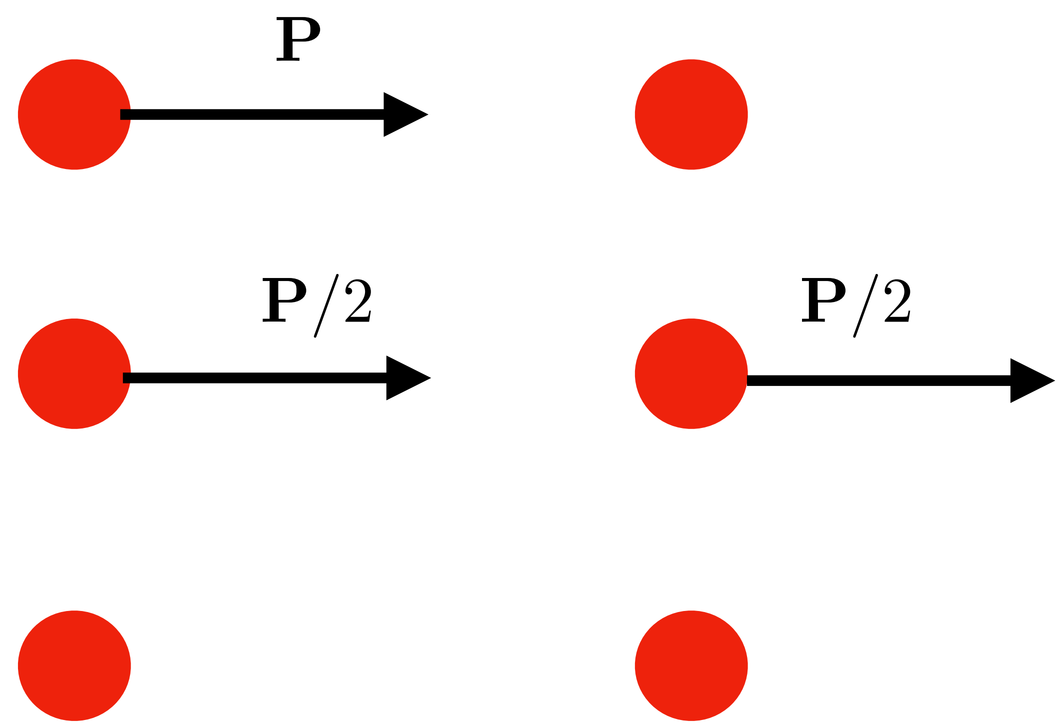

Potentials (breakup)

$$V^{\mathrm{LO}}_{x^{*4}=0}(\mathbf{x}_\perp) = \left.\frac{(L_\perp + L_\parallel)(\mathbf{x}, x^4, X^4)}{mG(\mathbf{x}, x^4, X^4)}\right|_{x^4=0,\mathbf{x}_\parallel=0} + \left.\frac{E(\mathbf{x}, x^4, X^4)}{G(\mathbf{x}, x^4, X^4)}\right|_{x^4=0,\mathbf{x}_\parallel=0}$$

Laplacian

energy

case1

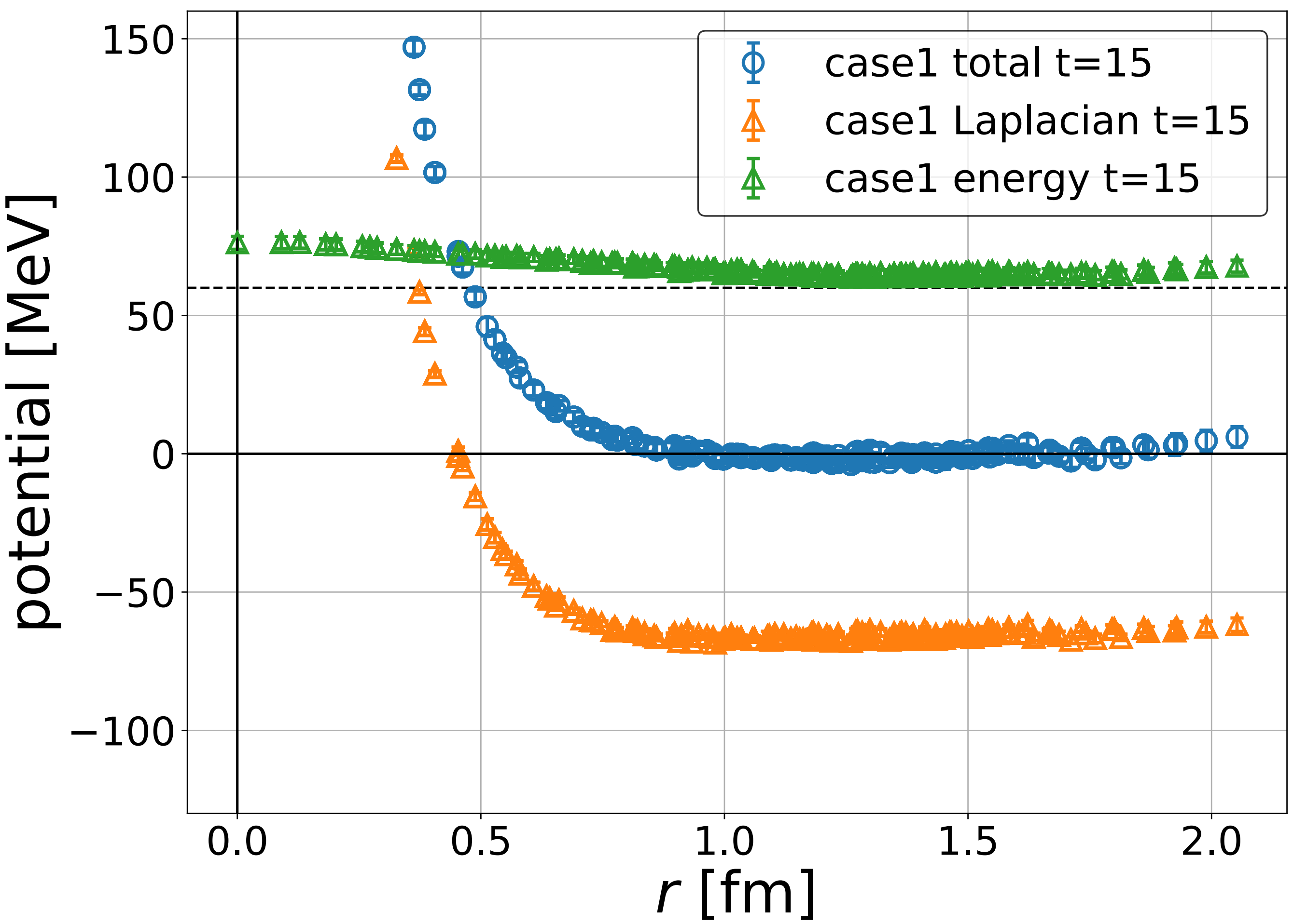

case2

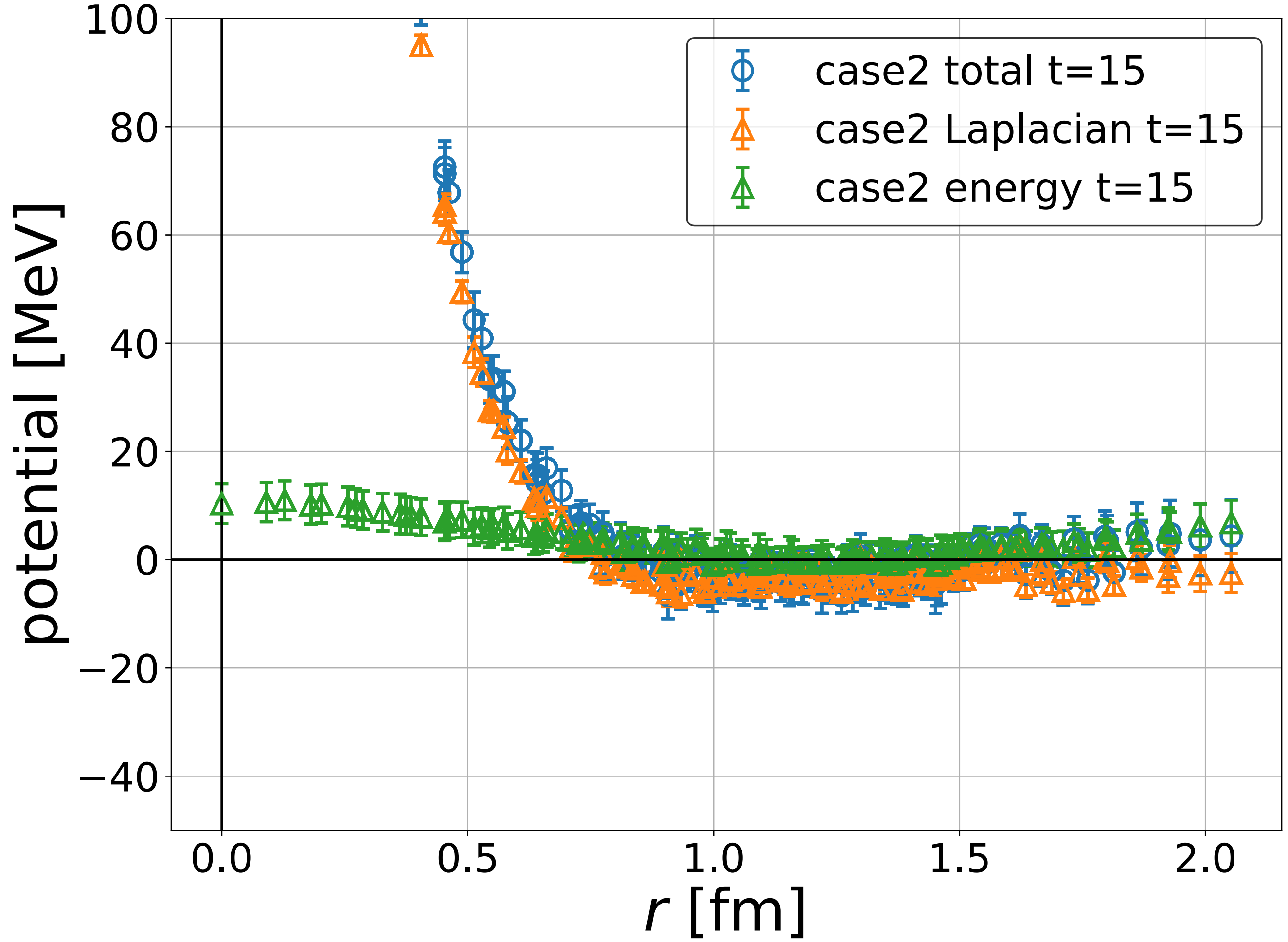

$\simeq$ CM

Potentials (comparison)

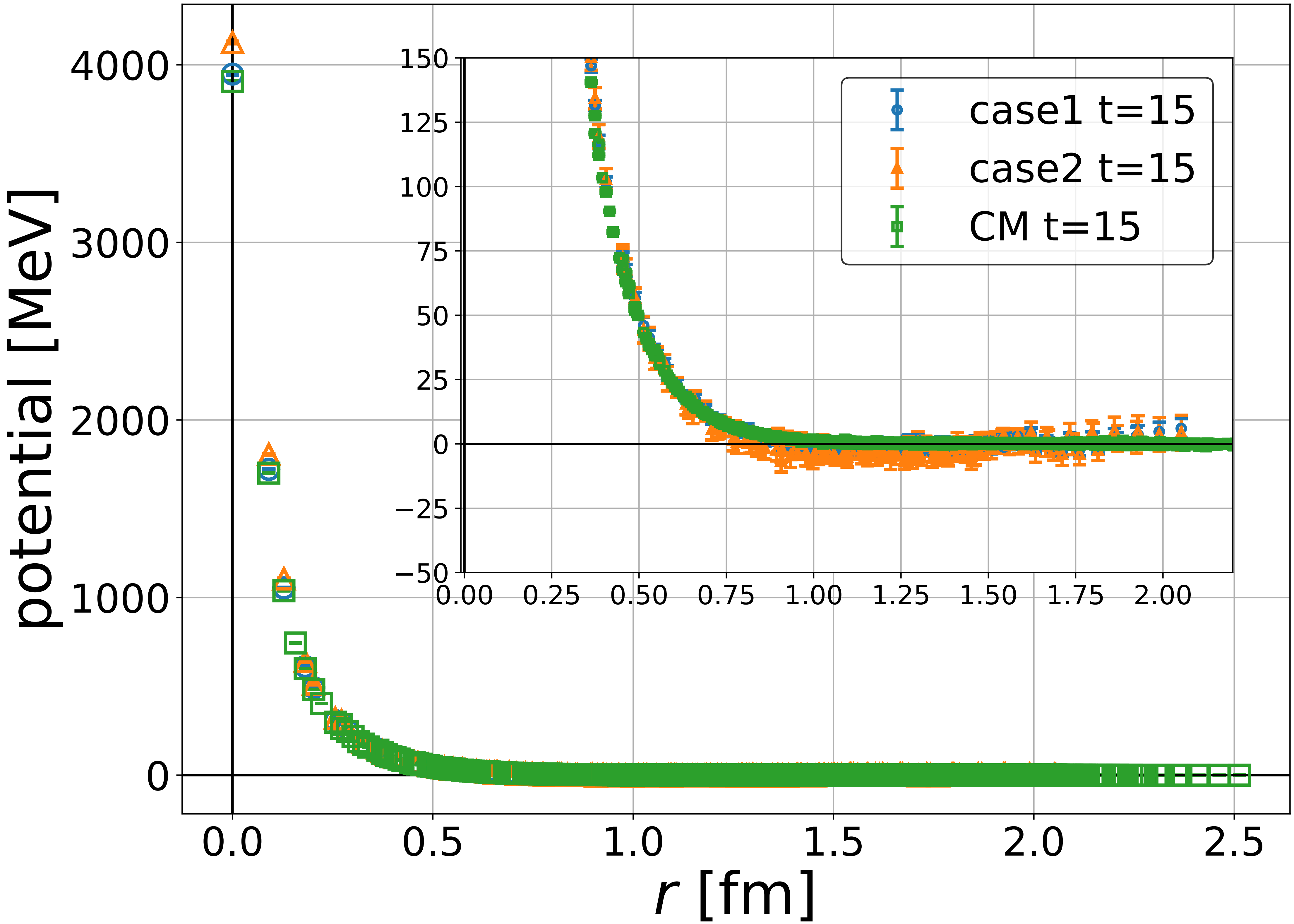

They are consistent except at short distances, though boosted ones are noisier.

Scattering phase shifts

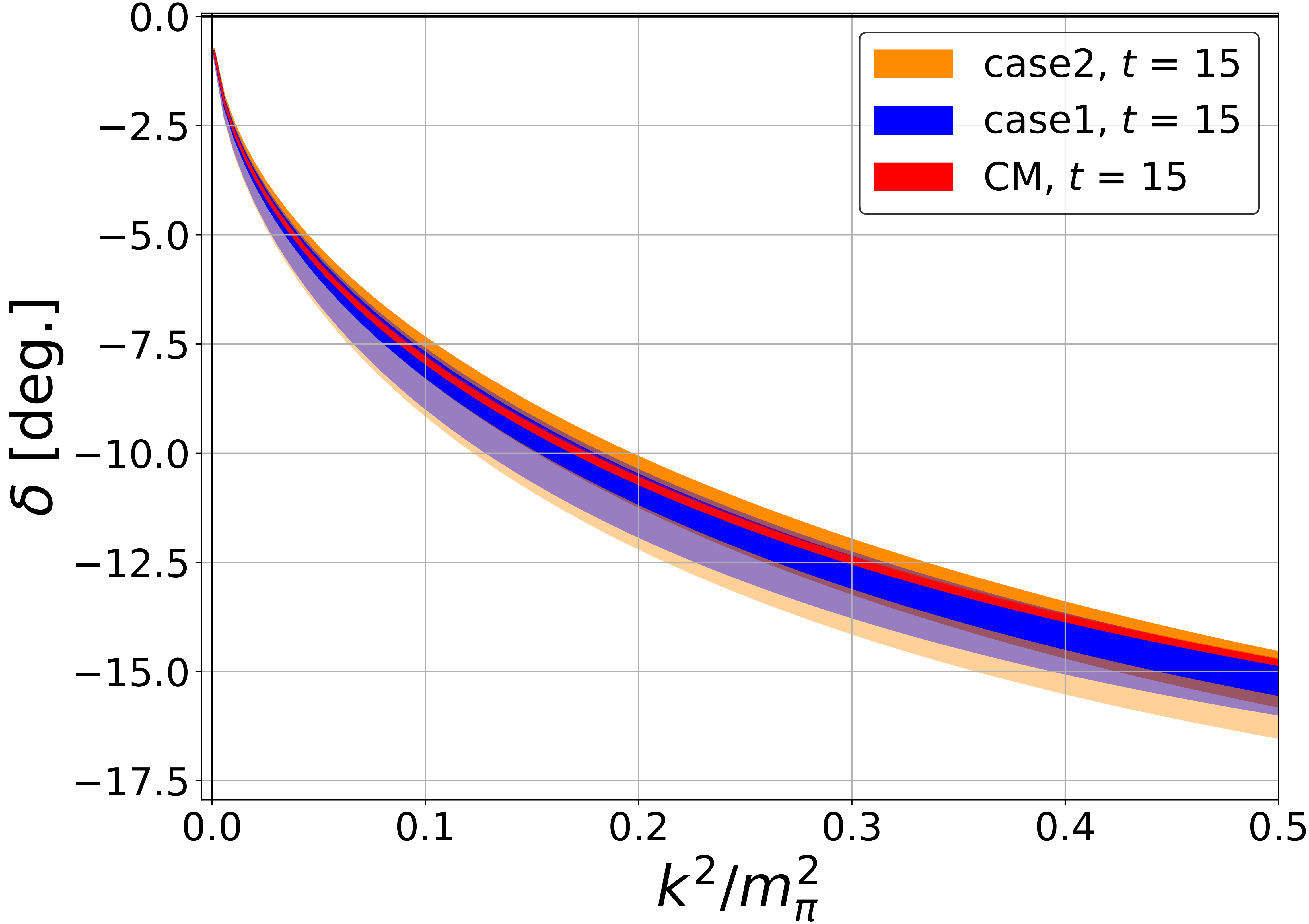

All three cases gives consistent results.

Finite volume spectra

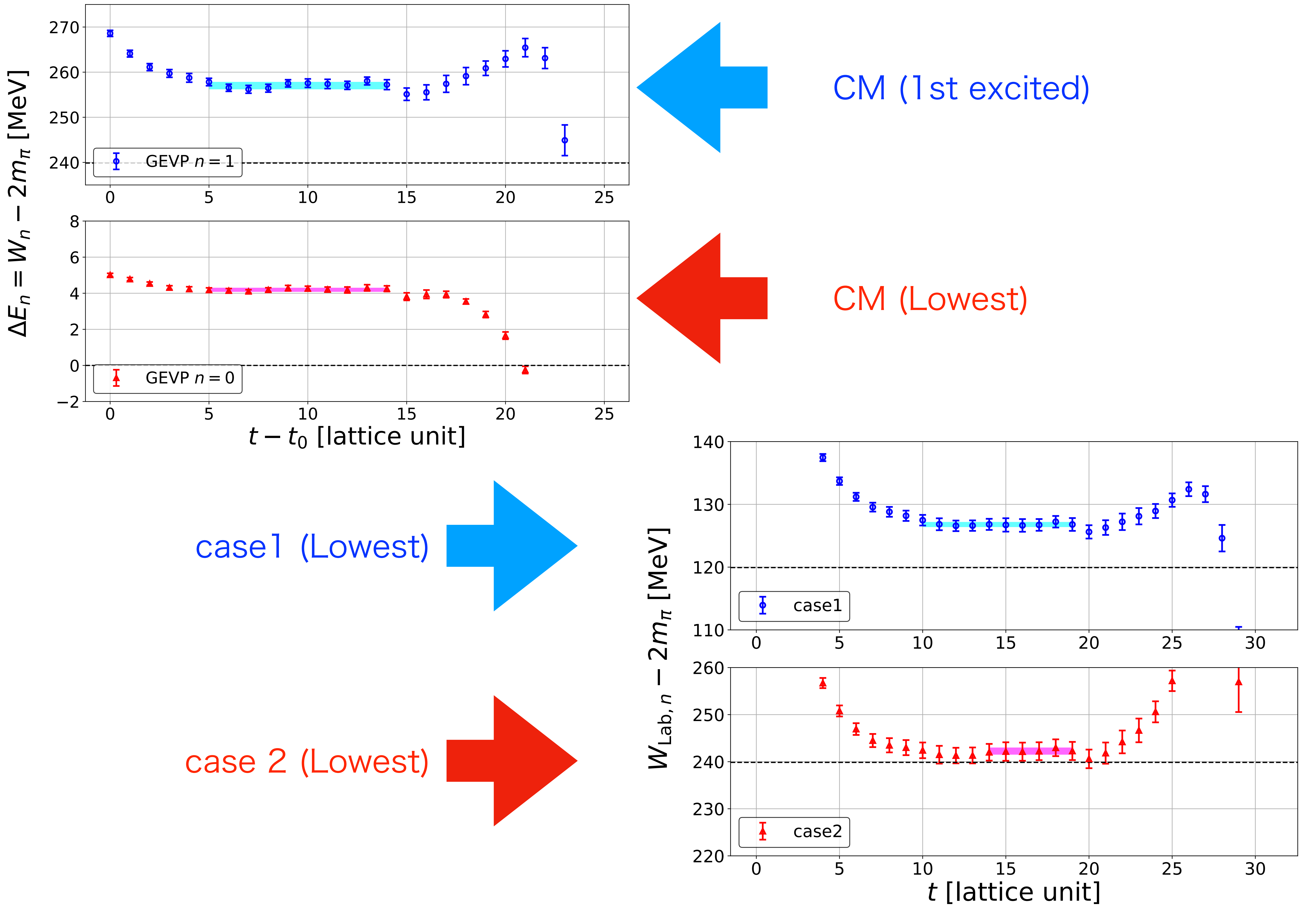

Comparison with finite volume method

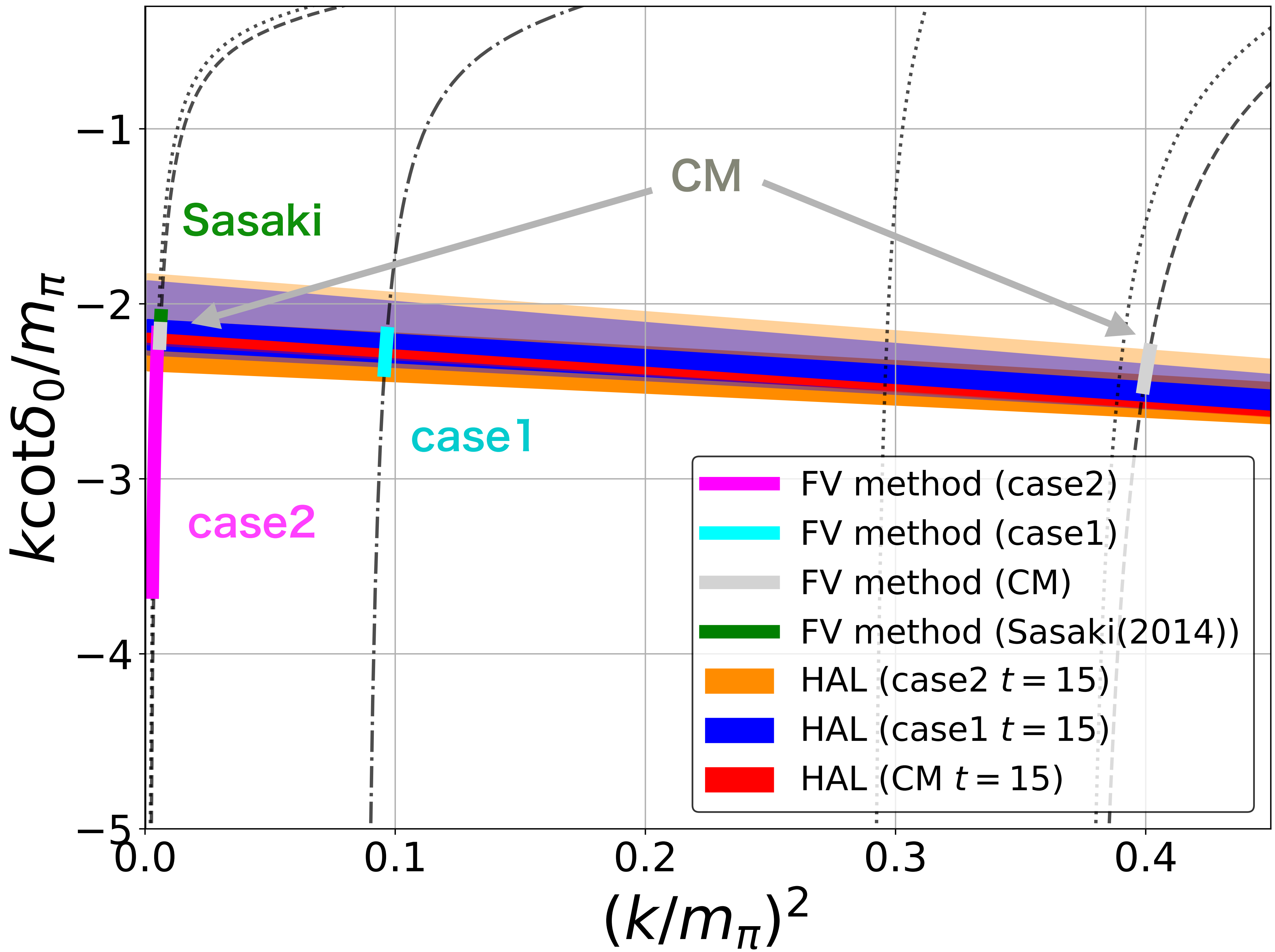

HAL QCD potentials with non-zero momentum work !

Comparison at low energies

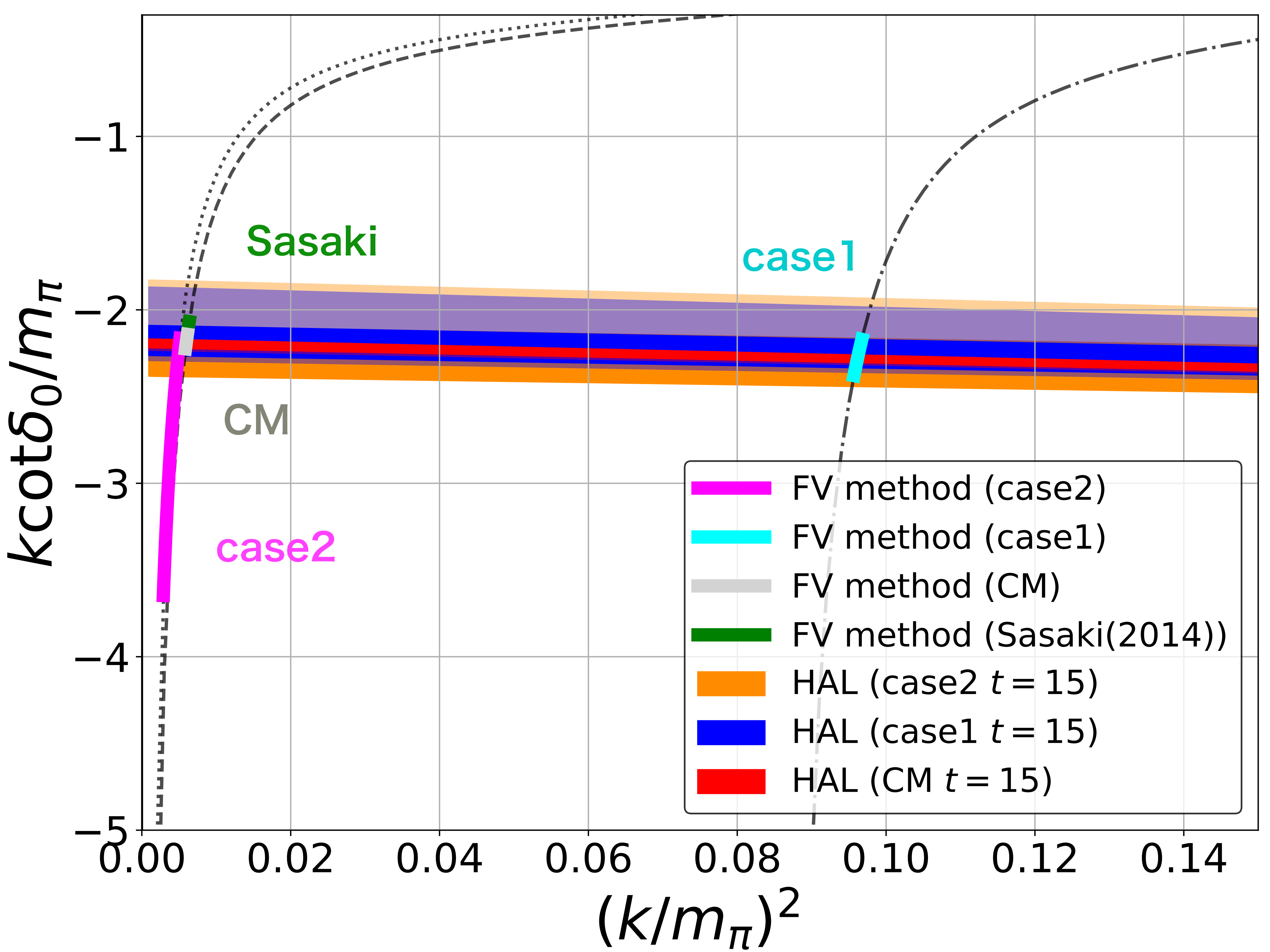

V. Summary and Discussions

- HAL QCD method provides useful tools to investigate not only dibaryons but also hadron resonates such as ρ meson.

- The formula to obtain potential in the HAL QCD method is extended to moving systems, and is shown to work for the $I = 2\pi\pi$ scattering.

HAL QCD method vs. finite volume spectra

A discrepancy that HAL QCD/FV spectra predict unbound/bound NN at $m_\pi \sim 700 - 800$ MeV recently seems to be resolved.

bound NN is disfavored.

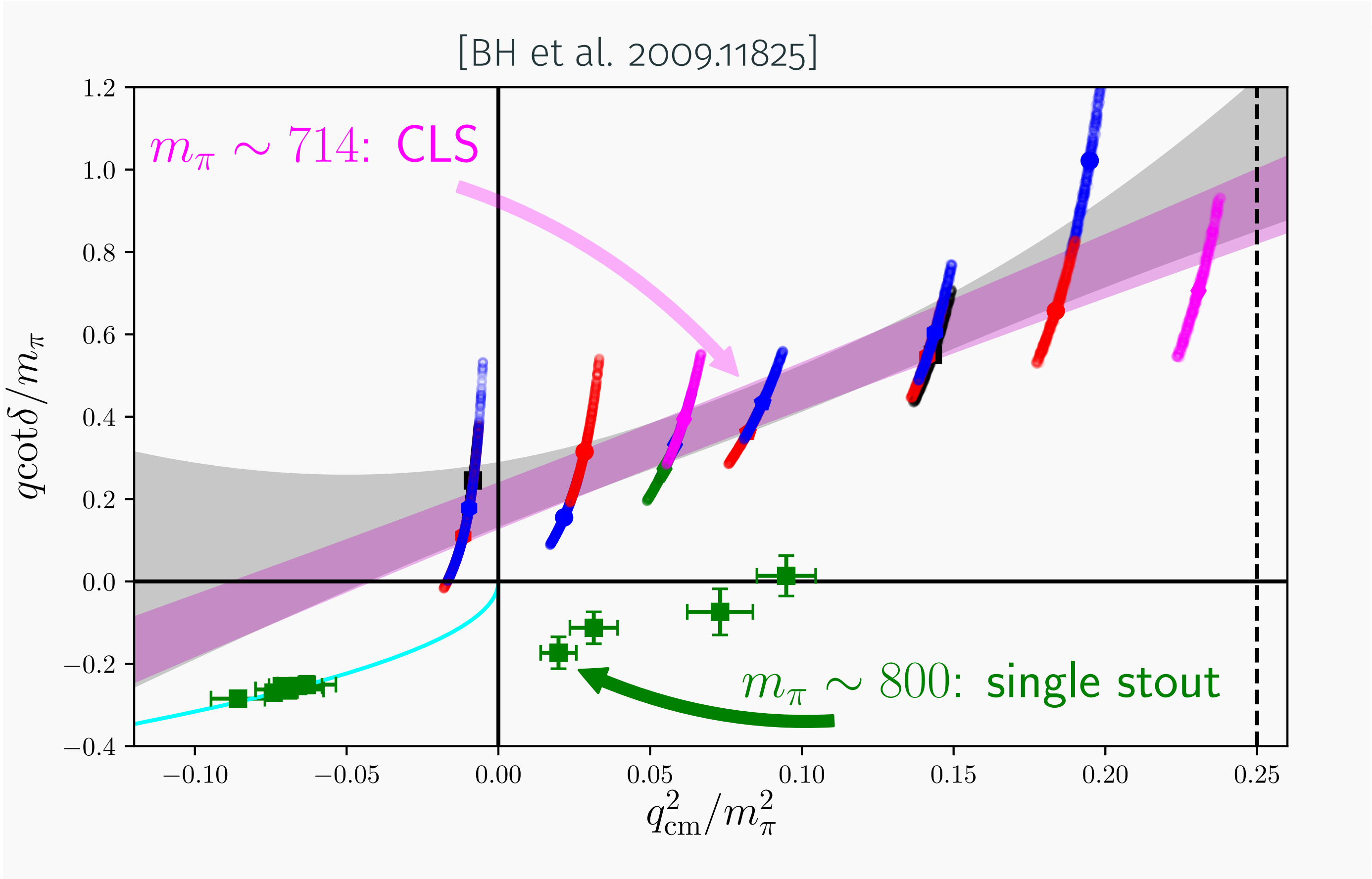

review by B. Hoerz in Lattice2021

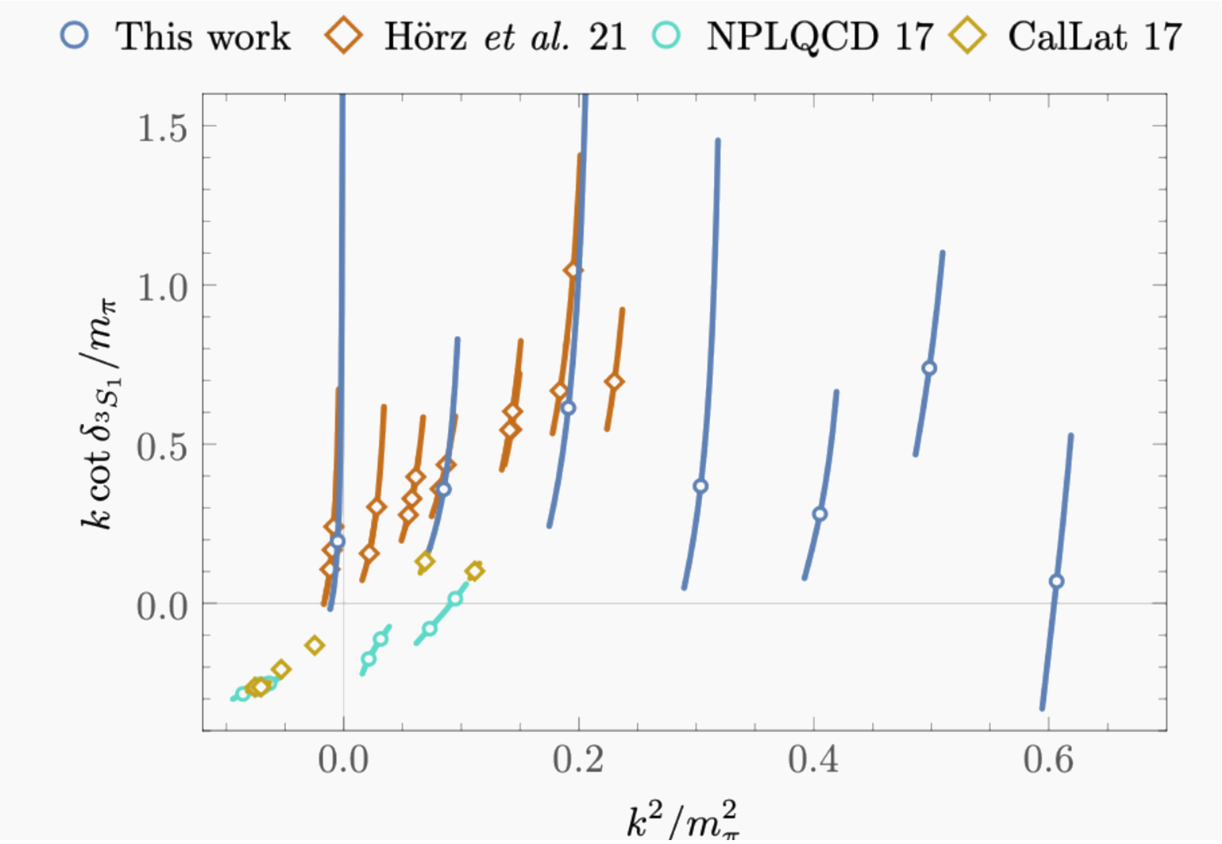

talk by M. Wagman in Lattice2021